Chemical Analyses

T-Hg in muscle and liver subsamples was analyzed using a flameless atomic absorption spectrophotometer (Hiranuma Sangyo, HG-1, Japan) after digestion by a mixture of HNO_3, $HClO_4$, and H_2SO_4 (Endo et al. 2002). DOLT-2 (National Research Council of Canada) was used as an analytical quality control of T-Hg as reported previously (Endo et al. 2009). The mean recovery of T-Hg from the quality control was 95 % ($n = 5$).

The stable isotope ratios of carbon ($\delta^{13}C$) and nitrogen ($\delta^{15}N$) in dried muscle samples, after removal of lipids using chloroform/methanol extraction, were analyzed using a mass spectrometer (Delta S; Finnigan, Germany) coupled with an elemental analyzer (EA1108; Fisons, Italy) as reported previously (Endo et al. 2009). CERKU-1, -2, and -5, certified by the Center for Ecology Research, Kyoto University (Kyoto, Japan), were used as $\delta^{13}C$ and $\delta^{15}N$ reference materials (Tayasu et al. 2011).

The TMF of T-Hg in star-spotted dogfish and spiny dogfish was calculated from the slope of the regression line generated from the $\delta^{15}N$ value and the logarithmic concentration of T-Hg in muscle or liver (Harmelin-Vivien et al. 2012).

Lipids in minced fresh liver samples were extracted three times by hexane. The combined extracts were concentrated and the HEL content determined gravimetrically (Hisamichi et al. 2012).

Statistical Analyses

Data were analyzed by Student t-test and Pearson's correlation coefficient test using the Statcell 2 program, with the level of significance at $p < 0.05$. The T-Hg data, shown in Figs. 1 and 4, were fitted to the Bèzier curve using KaleidaGraph (version 4.1, Hulinks Inc., Tokyo, Japan). All data are expressed as the means ± SDs.

Results

Total Body Length, Body Weight, Stable Isotope Ratios, Estimated Age, and Hg Concentrations in Muscle and Liver

Table 1 lists the analytical results for star-spotted dogfish purchased from the shark specialty store. The average body length of female fish (97 ± 4 cm) was significantly greater than that of male fish (88 ± 10 cm); the maximal body lengths of female and male specimens were 127 and 99 cm, respectively. The average body weight of female fish (3.6 ± 1.9 kg) was also significantly heavier than that of male fish (2.2 ± 0.7 kg). The estimated ages of the female and male specimens based on their body sizes were 8.8 ± 2.8 and 5.6 ± 1.3 years, respectively.

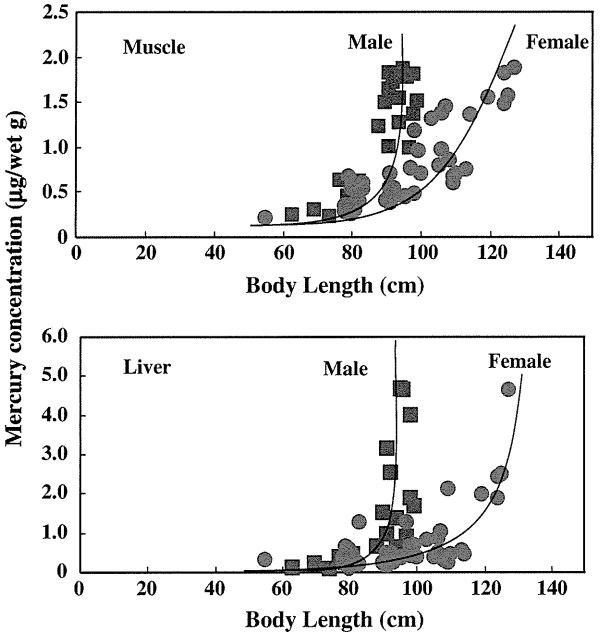

Fig. 1 Relationships between body length and Hg concentration in muscle or liver of male and female star-spotted dogfish

T-Hg concentrations in both muscle and liver samples from male fish were significantly greater than those from female fish ($p < 0.05$). Average T-Hg concentration in muscle samples was similar to that in liver samples, irrespective of sex, although the variation in T-Hg concentration in liver samples, as shown by the SDs, was greater than that in muscle samples. No differences were found in average $\delta^{15}N$ and $\delta^{13}C$ values in samples between male and female star-spotted dogfish.

Relationship Between Hg Concentrations in Muscle and Liver Samples and Body Length

The relationship between T-Hg concentration in muscle or liver samples and body length of star-spotted dogfish was investigated (Fig. 1). T-Hg concentrations in muscle samples from male and female fish increased with body length from approximately 80–90 cm, respectively, and the observed increases were more marked in male than in female fish. T-Hg concentrations in liver samples from male and female fish greatly increased with body lengths exceeding 90 and 110 cm, respectively, and increases in T-Hg observed in liver samples were more prominent than those in muscle samples: T-Hg concentrations were greater in liver than in muscle of most male dogfish specimens exceeding 90 cm and approximately half of female dogfish

Table 1 Analytical results for star-spotted dogfish caught off the northern region of Japan

Sex	Male ($n = 20$)	Female ($n = 41$)
Body length (cm)	88 ± 10 (63–99)	97 ± 4 (55–127)*
Body weight (kg)	2.2 ± 0.7 (0.9–3.2)	3.6 ± 1.9 (0.5–8.4)*
Hg concentration in muscle (μg/wet g)	1.15 ± 0.57 (0.202–1.841)	0.776 ± 0.460 (0.210–1.873)*
Hg concentration in liver (μg/wet g)	1.17 ± 1.73 (0.063–4.648)	0.607 ± 0.753 (0.063–4.642)*
$\delta^{13}C$ (‰)	−16.3 ± 0.4 (−17.5 to −15.9)	−16.2 ± 0.5 (−17.5 to −15.1)
$\delta^{15}N$ (‰)	12.5 ± 0.8 (11.0–13.7)	12.5 ± 0.8 (10.9–14.1)
Estimated age	5.6 ± 1.3 (3.8–7.9)	8.8 ± 2.8 (2.1–14.4)*

* Significantly different from male fish ($p < 0.05$)

specimens exceeding 110 cm, whereas the Hg concentration was lower in liver than in muscle of the smaller star-spotted dogfish specimens.

Relationships Among Stable Isotope Ratios, Hg Concentration, and Body Length

The relationship between $\delta^{15}N$ values in muscle samples and body length of star-spotted dogfish was next investigated (Fig. 2). $\delta^{15}N$ values in muscle samples from male and female star-spotted dogfish were significantly correlated with body length ($p < 0.05$), and the slopes of the regression lines were slightly steeper for the male samples than for the female samples. Although the data are not shown, $\delta^{13}C$ values in male and female dogfish specimens tended to be positively correlated with their body lengths ($p < 0.10$), and $\delta^{13}C$ values in male and female dogfish specimens, or in combined specimens, also tended to be positively correlated with their $\delta^{15}N$ values ($p < 0.10$).

The relationships between $\delta^{15}N$ value and T-Hg in muscle or liver samples of star-spotted and spiny dogfish species are shown in Fig. 3. The logarithmic concentrations of T-Hg in muscle samples from male and female star-spotted dogfish were significantly correlated with $\delta^{15}N$ values, and the slope of the regression lines of samples from male and female specimens were similar. Similarly, the logarithmic concentrations of T-Hg in liver samples from female star-spotted dogfish specimens were significantly correlated with $\delta^{15}N$ values ($p < 0.05$), whereas that from male specimens showed a slight correlation ($p < 0.10$). TMFs of T-Hg calculated from the slopes of the regression lines of male and female muscle specimens and female liver specimens ($p < 0.05$) were 1.63, 1.65, and 1.63, respectively, and the TMF calculated from the slope of the regression line of male liver samples ($p < 0.10$) was 1.98. Similar to star-spotted dogfish, the TMFs of T-Hg calculated from the slopes of the regressions lines of muscle specimens of male and female spiny dogfish ($p < 0.05$) were 1.35 and 1.82, respectively. The TMFs calculated from the slopes of the regression lines of liver specimens of male ($p > 0.10$) and female ($p < 0.05$) fish were 1.13 and 1.54, respectively, although most of the T-Hg concentrations in those specimens were near the detection limit of liver specimonts (0.05 μg/wet g).

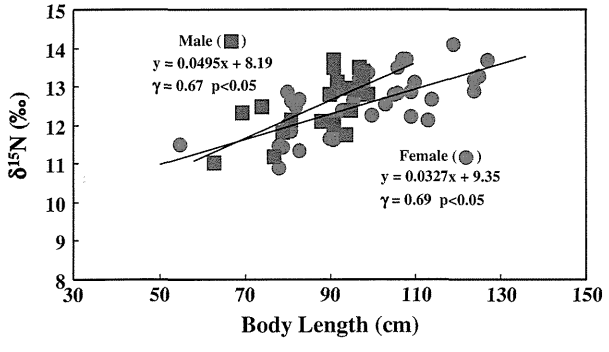

Fig. 2 Correlation between body length and $\delta^{15}N$ in muscle of male and female star-spotted dogfish

Comparison of Relationships Between Hg Concentrations in Muscle or Liver Samples and Estimated Age of Star-Spotted Dogfish with Those of Spiny Dogfish

The relationships between T-Hg concentration in muscle or liver samples and the estimated age of star-spotted dogfish were compared with those of spiny dogfish. The estimated ages of male and female spiny dogfish samples analyzed previously were 27 ± 7 years [range 16–41 ($n = 35$)] and 36 ± 11 years [range 18–61 ($n = 40$)], respectively (Endo et al. 2009), and those average ages were significantly older than the respective estimated ages of male and female star-spotted dogfish specimens listed in Table 1 ($p < 0.05$). However, body lengths of male and female spiny dogfish specimens (77.8 ± 10.8 and 94.9 ± 20.2 cm, respectively [Endo et al. 2009]) were similar to those of the respective star-spotted dogfish specimens (Table 1).

The relationships between T-Hg concentration in muscle or liver samples and the estimated age of star-spotted

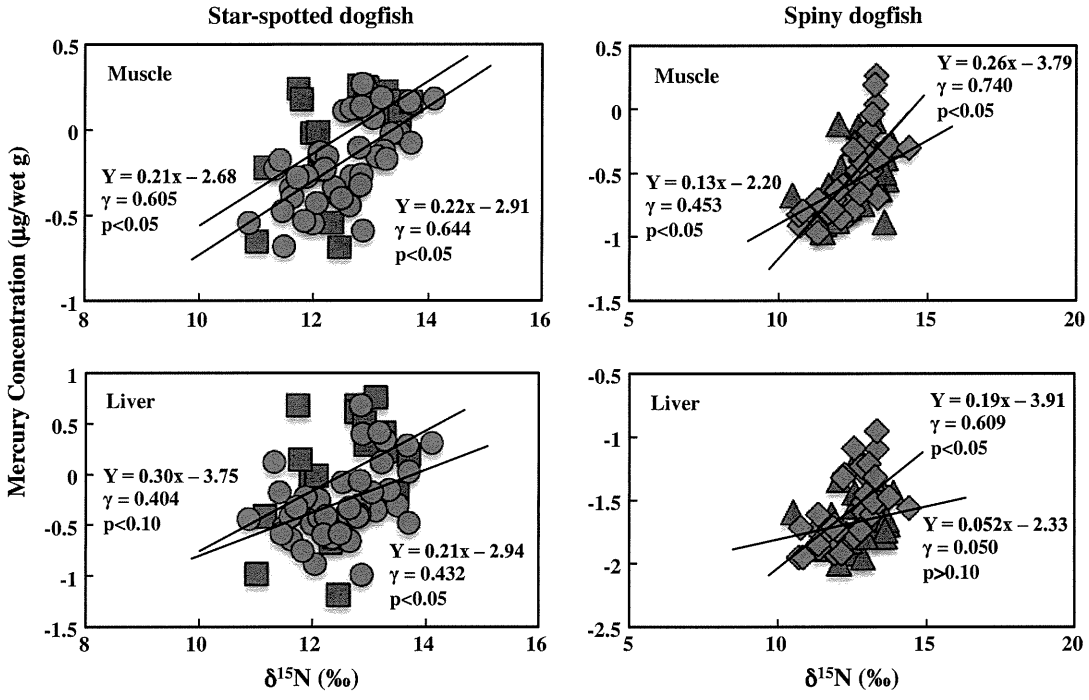

Fig. 3 Correlation between $\delta^{15}N$ and Hg concentration in muscle or liver of star-spotted and spiny dogfish

dogfish specimens differed markedly between male and female fish (Fig. 4) in a manner similar to the relationship between T-Hg concentration and body length (Fig. 1).

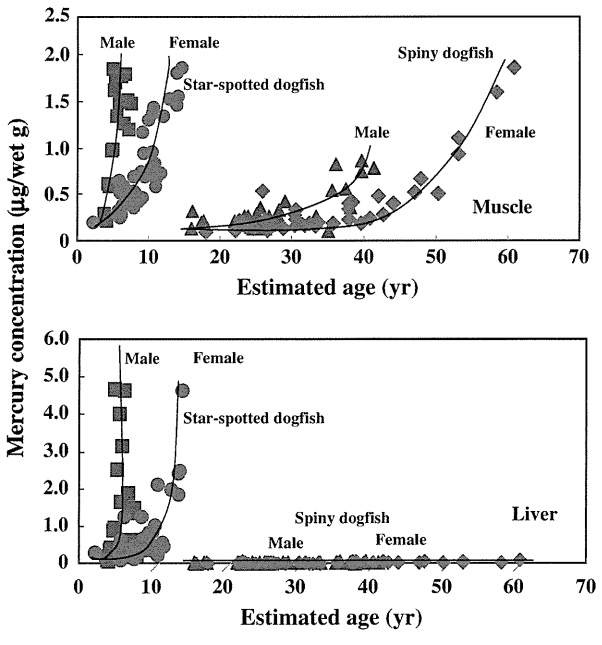

Fig. 4 Relationships between estimated age and Hg concentration in muscle or liver of male and female star-spotted dogfish. Hg concentrations in spiny dogfish are quoted from a previous report (Endo et al. 2009)

T-Hg concentrations in muscle samples from male star-spotted dogfish increased greatly from the estimated age of 3 or 4 years, and a less prominent increase in T-Hg was found in muscle samples from female dogfish. T-Hg concentrations in liver samples from male and female star-spotted dogfish markedly increased from the estimated ages of approximately 4 and 8 years, respectively, and the observed increase in male samples was more prominent than that in female samples. T-Hg concentrations in liver samples of male and female dogfish older than approximately 4 and 10 years, respectively, were greater than those in muscle samples.

Similar to star-spotted dogfish, the increase in T-Hg concentrations found in muscle samples of male spiny dogfish was more prominent than that in samples from female dogfish. However, these increases in T-Hg found in muscle samples from male and female spiny dogfish were moderate compared with the respective increases in T-Hg found in male and female star-spotted dogfish. It is worthy of note that T-Hg concentrations in liver samples from spiny dogfish were only trace (<0.11 μg/wet g), irrespective of sex, estimated age, and body length.

Although the data are not shown in figure, significant linear correlations ($p < 0.05$) were found between estimated ages and the logarithmic vales of T-Hg concentrations in muscle and liver samples except for hepatic T-Hg in male star-spotted dogfish samples ($p < 0.10$).

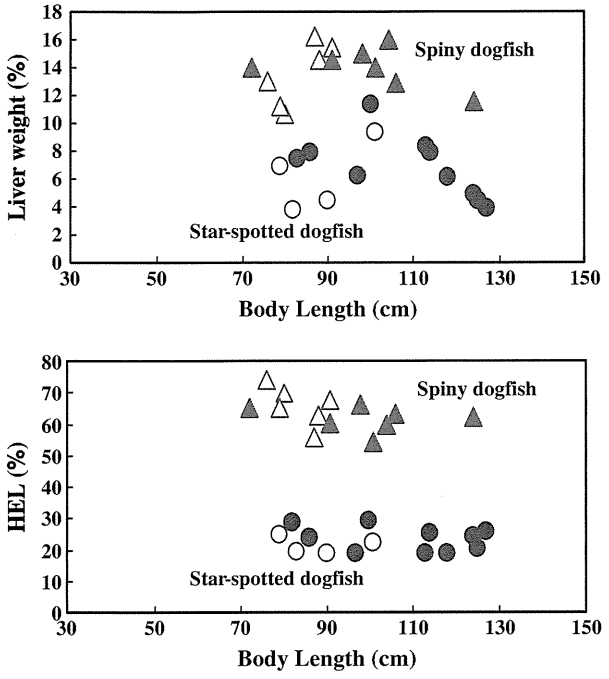

Fig. 5 Relationship between body length and relative liver weight or HEL content of star-spotted and spiny dogfish. *Open symbols* male, *closed symbols* female

Hepatic Weight and HEL Content in Liver of Star-Spotted and Spiny Dogfish

Hepatic weight and HEL content of star-spotted dogfish (4 male and 10 female) were compared with those of spiny dogfish (6 male and 8 female) (Fig. 5). No sex differences were observed in the ratio of hepatic weight to body weight or HEL content in either dogfish species, although the number of male star-spotted dogfish ($n = 4$) was limited, and no growth-related changes were observed in either liver weight or HEL content. Ratios of liver weight and HEL content in combined star-spotted dogfish specimens ($n = 14$) were 6.90 ± 2.73 % and 22.7 ± 3.7 %, respectively. In contrast, the ratios of liver weight and HEL content in combined male and female spiny dogfish specimens ($n = 14$) were 13.6 ± 2.2 % and 63.5 ± 5.4 %, respectively. Both ratios of liver weight and HEL content in star-spotted dogfish specimens were significantly lower than those in spiny dogfish specimens ($p < 0.05$), respectively.

Discussion

A marked increase in T-Hg in muscle samples from male fish and a less prominent increase in T-Hg in those from female fish were found in star-spotted dogfish specimens (Fig. 1). These results were similar to those previously observed in spiny dogfish (Forrester et al. 1972; Ketchen 1975; Endo et al. 2009), shortspine dogfish (Taguchi et al. 1979), and other shark species (Lyle et al. 1984). The difference in T-Hg increases between male and female fish can be explained by the continuous intake of Hg by way of food consumption, the cessation of growth at maturity, and the slower growth rate of male fish (Forrester et al. 1972; Ketchen 1975; Taguchi et al. 1979; Lyle 1984; Endo et al. 2009). T-Hg concentrations in muscle samples (edible portion) of larger male and female star-spotted dogfish (larger than approximately 85 and 105 cm, respectively) exceeded 1.0 μg/wet g (Fig. 1). Methylmercury (Me-Hg) appears to be the predominant form of Hg in muscle of star-spotted dogfish as well as in that of other fish species (Storelli and Marcotrigiano 2002; Hisamichi et al. 2012) and cetaceans (Endo et al. 2002, 2008b). Thus, the Me-Hg concentration in muscle of larger star-spotted dogfish may exceed 1.0 μg/wet g, which is the United States Food and Drug Administration action level and Codex Alimentarius guideline level for Me-Hg in predatory fish.

The increases in T-Hg found in liver of male and female star-spotted dogfish were both more marked and occurred slightly later than increases in T-Hg observed in muscle samples (Fig. 1). The marked increases of T-Hg in liver samples may be explained by the cessation of growth at maturity as well as the formation of mercury selenide (HgSe) in liver after the demethylation of Me-Hg (Endo et al. 2002; Storelli and Marcotrigiano 2002; Endo et al. 2005). We initially analyzed Me-Hg in liver and muscle samples from randomly selected male ($n = 4$) and female ($n = 4$) star-spotted dogfish: The percentages of Me-Hg/T-Hg in liver and muscle samples ranged from 3 to 14 % and 59 to 74 %, respectively. The results of the preliminary analysis agree with the previous results for Hg speciation in spiny dogfish (Endo et al. 2009) and cetaceans (Endo et al. 2004, 2005, 2008b), suggesting that the major Hg species in liver and muscle samples from star-spotted dogfish are inorganic Hg (probably in the form of HgSe) and Me-Hg, respectively. To confirm the formation of HgSe in liver of star-spotted dogfish, determination of Me-Hg as well as Se is necessary. Little information concerning the formation of HgSe in the liver of shark species is available (Storelli and Marcotrigiano 2002; Branco et al. 2007), and, apart from our studies of tiger sharks (Endo et al. 2008a) and spiny dogfish (Endo et al. 2009), no comparative analyses of Hg in liver and muscle of shark species at various stages of growth have been reported to date. Most studies focusing on the formation of HgSe have investigated liver of cetaceans containing high levels of T-Hg and Se (Endo et al. 2002, 2005, 2008b), and those studies reported a marked increase of T-Hg in liver tissue alone. To our knowledge, the present study is the first report to show a prominent

increase in T-Hg in liver that occurs slightly later than T-Hg increases in muscle. Further study focusing on growth stage and Hg and Se speciation in liver as well as muscle is necessary.

Compared with the marked increases in T-Hg in liver of male and female star-spotted dogfish specimens (Fig. 4), only trace levels of T-Hg were found in liver specimens of spiny dogfish, irrespective of body length and estimated age. In agreement with our results, Greig et al. (1977) reported a lower T-Hg concentration in liver than in muscle of spiny dogfish. The marked differences in HEL content and hepatic weight between star-spotted and spiny dogfish (Fig. 5) may explain the differences in hepatic T-Hg concentrations between the two dogfish species, and the larger liver in spiny dogfish, which contains large amounts of oil, explains why this shark liver is used as raw material for liver oil. To our knowledge, hepatic lipid content and hepatic size have not been studied in association with Hg distribution in animals. Balshaw et al. (2008) and Hisamichi et al. (2012) suggested that the low T-Hg concentration found in farmed tuna muscle is due to the presence of a high level of lipids, and Haraguchi et al. (2000) reported trace levels of T-Hg in blubber of cetacean products. Available data for other shark species variously indicate greater concentrations of T-Hg in muscle than in liver (Greig et al. 1977; Branco et al. 2007) as well as similar levels of T-Hg in muscle and liver (Marcovecchi et al. 1991). We recently reported a lower concentration of T-Hg in liver than in muscle of immature tiger sharks and a greater concentration of T-Hg in mature sharks (Endo et al. 2008a). However, none of these studies analyzed hepatic size or lipid content. Studies of the relationship between lipid content in liver and Hg distribution in other shark species are now in progress.

In general, Hg accumulation in predatory species is correlated with increases in age rather than body length (Ketchen 1975; Taguchi et al. 1979; Honda et al. 1983) and tends to be greater in animals with slower growth rate (Ketchen 1975; Greig et al. 1977; Taguchi et al. 1979; Lyle 1984). In the present study, the relationship between estimated age and T-Hg concentration in muscle or liver (Fig. 4) indicates species differences in T-Hg accumulation between the star-spotted and spiny dogfish species, although the relationships between body length and T-Hg concentrations in muscle from both species are similar (figure not shown). Contrary to expectations, T-Hg concentrations in muscle and liver from spiny dogfish samples (Endo et al. 2009) were lower than those from star-spotted dogfish of similar body length (Table 1), despite the longer life span and slower growth rate of the former species. Average $\delta^{13}C$ values in samples from male and female star-spotted dogfish (Table 1) were greater than those from male and female spiny dogfish (-17.3 ± 0.4 and -17.2 ± 0.4 ‰, respectively [Endo et al. 2009]). The greater $\delta^{13}C$ values may reflect the coastal or benthic prey consumed by the star-spotted dogfish compared with the offshore or pelagic prey of the spiny dogfish (Kelly 2000). Differences in feeding ecology, hepatic size, and hepatic oil content may also be reasons for the lower T-Hg contamination in spiny dogfish than in star-spotted dogfish.

Average $\delta^{13}C$ and $\delta^{15}N$ values in samples from male star-spotted dogfish were similar to those from female dogfish despite marked differences in body length and estimated age (Table 1). The slopes of the regression lines generated from the plots of body length versus $\delta^{15}N$ values for star-spotted dogfish specimens were slightly steeper for male fish ($y = 0.0495x + 8.19$, $p < 0.05$) than for females fish ($y = 0.0327x + 9.35$, $p < 0.05$) (Fig. 2). Average $\delta^{15}N$ values and body lengths in samples from male and female spiny dogfish (Endo et al. 2009) were similar to those from male and female star-spotted dogfish samples (Table 1), respectively, and the slope of the regression line calculated from the body length and $\delta^{15}N$ values for spiny dogfish specimens was also slightly steeper for male fish ($y = 0.0381x + 9.41$, $p < 0.05$) than for female fish ($y = 0.0277x + 9.74$, $p < 0.05$) (Endo et al. 2009). The slower growth rate for male fish versus female fish in both dogfish species may explain the small differences observed in the slopes.

TMFs of T-Hg calculated from muscle samples from male (1.63) and female (1.65) star-spotted dogfish specimens were very similar. These similarities in TMFs, as well as in $\delta^{13}C$ and $\delta^{15}N$ values, between male and female samples may suggest a similar trophic position and feeding ecology in male and female fish, again despite marked differences in the body length and age of specimens analyzed. Similar $\delta^{13}C$ and $\delta^{15}N$ values were also found in male and female spiny dogfish (Endo et al. 2009), but the TMF of T-Hg calculated from muscle samples from male fish (1.35) was different from that of female fish (1.82). Differences in the range of estimated ages of male (16–41 years) and female fish (18–61 years) may provide a possible explanation for this difference. Interestingly, similar TMFs of T-Hg were reported from the slope of the regression line generated by the $\delta^{15}N$ value and the log-transformed T-Hg concentration in muscle of European hake of different body lengths (1.675 [Harmelin-Vivien et al. 2012]) as well as from the slopes of the regression lines of marine food webs of the Arctic (1.57 [Campbell et al. 2005]) and Brazil (1.17–1.67 [Bisi et al. 2012]).

In conclusion, T-Hg concentrations in muscle and liver of male star-spotted dogfish specimens were greater than those in muscle and liver of female specimens of a similar body length, reflecting the slower growth rate of male fish. Prominent increases in T-Hg concentrations in liver of male and female star-spotted dogfish specimens due to the

formation of HgSe were found to occur slightly later than increases in T-Hg concentrations in their muscles. The body length and weight of male and female star-spotted dogfish specimens, as well as the $\delta^{15}N$ values analyzed in this study, were similar to those of male and female spiny dogfish specimens analyzed in a previous study (Endo et al. 2009). However, T-Hg concentrations in liver of male and female spiny dogfish specimens were drastically lower than those of star-spotted dogfish specimens, and liver weight and HEL content of the former were significantly higher than those of the latter. These differences in liver weight and HEL content may explain the marked difference in hepatic T-Hg accumulation between the two dogfish species. Further comparative study is necessary to elucidate the differences in T-Hg concentrations in muscle and liver based on growth rate and growth stage, liver size and oil content, and feeding preference.

Acknowledgments This work was supported by Grants-in-Aid from the Japan Society for the Promotion of Science (Grants No. B24310049 and C21590135). Stable isotope analyses were performed using a Joint Use/Research Grant of Center for Ecological Research, Kyoto University (Kyoto, Japan).

References

Balshaw S, Edwards JW, Ross KE, Daughtry BJ (2008) Mercury distribution in the muscular tissue of farmed southern bluefin tuna (*Thunnus maccoyii*) is inversely related to the lipid content of tissue. Food Chem 111:616–621

Bisi TL, Lepont G, Azevedo ADF, Dorneles PR, Flach L, Das K et al (2012) Trophic relationships and mercury biomagnification in Brazilian tropical coastal food webs. Ecol Indic 18:291–302

Branco V, Vale C, Canário J, dos Santos MN (2007) Mercury and selenium in blue shark (*Prionace glauca*, K. 1758) and swordfish (*Xiphias gladius*, L. 1758) from two areas of the Atlantic Ocean. Environ Pollut 150:373–380

Campbell LM, Norstrom RJ, Hobson KA, Muir DCG, Backus S, Fisk AT (2005) Mercury and other trace elements in a pelagic Arctic marine food web (Northwater Polynya, Baffin Bay). Sci Total Environ 351–352:247–263

Endo T, Haraguchi K, Sakata M (2002) Mercury and selenium concentrations in the internal organs of toothed whales and dolphins marketed for human consumption in Japan. Sci Total Environ 300:15–22

Endo T, Haraguchi K, Cipriano F, Simmonds MP, Hotta Y, Sakata M (2004) Contamination by mercury and cadmium in the cetacean products from Japanese market. Chemosphere 54:1653–1662

Endo T, Haraguchi K, Hotta Y, Hisamichi Y, Lavery S, Dalebout ML et al (2005) Total mercury, methyl mercury and selenium levels in the red meat of small cetaceans sold for human consumption in Japan. Environ Sci Technol 3:5703–5708

Endo T, Hisamichi Y, Haraguchi K, Kato Y, Ohta C, Koga N (2008a) Hg, Zn and Cu levels in the muscle and liver of tiger sharks (*Galeocerdo cuvier*) from the coast of Ishigaki Island, Japan: relationship between metal concentrations and body length. Mar Pollut Bull 56:1774–1780

Endo T, Hisamichi Y, Kimura O, Haraguchi K, Baker CS (2008b) Contamination levels of mercury and cadmium in melon-headed whales (*Peponocephala electra*) from a mass stranding on the Japanese coast. Sci Total Environ 401:73–80

Endo T, Hisamichi Y, Kimura O, Kotaki Y, Kato Y, Ohta C et al (2009) Contamination levels of mercury in the muscle of female and male of spiny dogfishes (*Squalus acanthias*) caught off the coast of Japan. Chemosphere 77:1333–1337

Forrester CR, Ketchen KS, Wong CC (1972) Mercury content of spiny dogfish (*Squalus acanthias*) in the Strait of Georgia, British Columbia. J Fish Res Board Can 29:1487–1490

Greig RA, Wenzloff D, Shelpuk C, Adams A (1977) Mercury concentrations in three species of fish from North Atlantic offshore waters. Arch Environ Contam Toxicol 5:315–323

Haraguchi K, Endo T, Sakata M, Masuda Y (2000) Contamination survey of heavy metals and organochlorine compounds in cetacean products purchased in Japan. J Food Hyg Soc Japan 41:287–296

Harmelin-Vivien M, Bodiguel X, Charmasson S, Loizeau V, Mellon-Ducal C, Tronczynski J et al (2012) Differential biomagnification of PCB, PBDE, Hg and radiocesium in the food web of the European hake from the NW Mediterranean. Mar Pollut Bull 64:974–983

Hisamichi Y, Haraguchi K, Endo T (2012) Levels of mercury and organohalogen compounds in Pacific bluefin tuna (*Thunnus orientallis*) cultured at different regions of Japan. Arch Environ Contam Toxicol 62:296–305

Honda K, Tatsukawa R, Itano K, Miyazaki N, Fujiyama T (1983) Heavy metal concentrations in muscle, liver and kidney tissue of striped dolphins, *Stenella coeruleoalba*, and their variation with body length, weight, age and sex. Agric Biol Chem 47: 1219–1228

Kelly JF (2000) Stable isotopes of carbon and nitrogen in the study of avian and mammalian trophic ecology. Can J Zool 78:1–27

Ketchen KS (1975) Age and growth of dogfish *Squalus acanthias* in British Columbia waters. J Fish Res Board Can 32:43–59

Lyle JM (1984) Mercury concentrations in four carcharhinid and three hammerhead sharks from coastal waters of the northern territory. Aust J Mar Freshw Res 35:441–451

Marcovecchi JE, Moreno VJ, Pérez A (1991) Metal accumulation in tissues of sharks from the Bahia Balanca estuary, Argentina. Mar Environ Res 31:263–274

Storelli MM, Marcotrigiano GO (2002) Mercury speciation and relationship between mercury and selenium in liver of *Galeus melastomus* from the Mediterranean Sea. Bull Environ Contam Toxicol 69:516–522

Taguchi M, Yasuda K, Toda S, Shimizu M (1979) Study of metal contents of elsmobranch fishes: part 1—Metal concentration in the muscle tissue of dogfish *Squalus mitsukurii*. Mar Environ Res 2:239–249

Tanaka A, Mizue K (1979) Studies on sharks. XV. Age and growth of Japanese dogfish *Mustelus manazo* bleeker in the East China Sea. Bull Japan Soc Sci Fish 45:43–50

Taniuchi T, Kuroda N, Nose Y (1983) Age, growth and reproduction and food habits of star-spotted dogfish *Mustelus manazo* collected from Choshi. Bull Japan Soc Sci Fish 49:1325–1334

Tayasu I, Hirasawa R, Ogawa NO, Ohkouchi N, Yamada K (2011) New organic reference materials for carbon- and nitrogen-stable isotope ratio measurements provided by Center for Ecological Research, Kyoto University, and Institute of Biogeosciences, Japan Agency for Marine-Earth Science and Technology. Limnology 12:261–266

Screening for Antibodies to Human T-Cell Leukemia Virus Type I in Japanese Breast Milk

Futoshi Matsubara,*[a] Koichi Haraguchi,[b] Kouji Harada,[c] and Akio Koizumi[c]

[a] *Department of Microbiology and Biochemistry, Daiichi College of Pharmaceutical Sciences;* [b] *Department of Analytical Chemistry, Daiichi College of Pharmaceutical Sciences; 22–1 Tamagawa-cho, Minami-ku, Fukuoka 815–8511, Japan: and* [c] *Department of Health and Environmental Sciences, Graduate School of Medicine, Kyoto University; Yoshida, Sakyo-ku, Kyoto 606–8501, Japan.* Received August 2, 2011; accepted February 1, 2012

Japanese breast milk samples were tested for antibodies to human T-cell leukemia virus type I (HTLV-1) by particle agglutination (PA) and a line immunoassay (LIA). In the PA method, the agglutination reaction between the HTLV-1 antibody and sensitized particles occurred at a 1 : 128 dilution of some breast milk samples. The average antibody titer was one order of magnitude lower than that in the serum positive control. A total of 243 human breast milk specimens were assayed by PA, of which 21 samples from Okinawa, Hyogo, Miyagi and Hokkaido were positive or deferred. The results of the 21 positive samples were subsequently assayed by LIA (INNO-LIA™ HTLV I/II) for confirmation; and one sample was positive, and two were indeterminate. We attempted to use polymerase chain reaction (PCR) to detect HTLV-1 provirus DNA, but we did not detect PCR products for the pX1 region of the HTLV-1 genome in the LIA-positive samples. These negative PCR results are most likely due to the lower sensitivity of the PCR for amplification from milk than from HTLV-1-positive monocytes. In conclusion, the PA method to breast milk samples appears to be a suitable tool to screen for antibodies to HTLV-1 in the breast milk of carrier mothers in cases in which it would be difficult to use serum for the test. Although LIA may be able to confirm HTLV-1 infection, the presence of HTLV-1 provirus should be confirmed in the breast milk.

Key words human T-cell leukemia virus type I; breast milk; particle agglutination; polymerase chain reaction; Western blotting

Adult T-cell leukemia (ATL) is a malignant tumor of CD4-positive T cells that is caused by infection with human T-cell leukemia virus type I (HTLV-1). When the RNA genome of HTLV-1, a retrovirus, enters target cells, the corresponding DNA is integrated into the host genome as a provirus by reverse transcription.[1–3] In ATL-endemic areas, the percentage of HTLV-1 carriers is high. Both HTLV-1 and ATL have been shown to be endemic in southwest Japan, the Caribbean islands, South Americas, and parts of Central Africa.[4–6] Antibodies against HTLV-1 have been found in over one million individuals, and more than 700 cases of ATL have been diagnosed each year in Japan alone. The cumulative incidence of ATL among HTLV-1 carriers in Japan is estimated to be 2.5% (3–5% in males, 1–2% in females).[7] The three major routes of transmission for HTLV-1 are blood transfusion, sexual contact and mother-to-child transmission. Mother-to-child transmission is a vertical transmission and occurs *via* breast milk.[4]

Vertical transmission occurs *via* infection of the lymphocytes in breast milk.[5,6] Individuals who are positive for anti-HTLV-1 antibodies are carriers of HTLV-1. The breast milk of carrier mothers (HTLV-1 sero-positive mothers) must not be fed to infants to prevent transmission. The presence of HTLV-1 infection can be determined by testing for HTLV-1 antibodies in serum samples. As a screening test for serum antibodies, particle agglutination (PA) has typically been performed. This method is based on the agglutination reaction between particles coated with HTLV-1 antigens and antibodies in the test sample.[7] To confirm the detection of HTLV-1 antibodies in pregnant women, enzyme-linked immunosorbent assays (ELISA) with disrupted whole viruses, synthetic peptides, or recombinant proteins; indirect immunofluorescence (IF) assays; and Western blot assays such as line immunoassays (LIAs) have been considered.[8,9] Recently, a high-throughput nucleic acid testing system was developed to detect proviral HTLV-1 DNA using an automatic nucleic acid extractor and real-time TaqMan polymerase chain reaction (PCR) targeting the pX region of the HTLV-1 genome.[10]

Human breast milk samples are a direct source of infection and can be sampled non-invasively. Kinoshita *et al.*[11] demonstrated the presence of the HTLV-1 antigen in milk from three sero-positive mothers using an IF method. However, screening and confirmatory tests for the presence of HTLV-1 antibodies in breast milk samples have not been considered.

The objective of this study is to determine whether it is possible to directly detect anti-HTLV-1 antibodies in breast milk instead of serum from carrier mothers. We initially used the PA-screening method to detect anti-HTLV-1 antibodies in Japanese breast milk samples collected in ten districts. Subsequently, we confirmed the results for the PA-positive samples using LIA for the detection of the HTLV-1 antibody. In addition, PCR was used to detect provirus HTLV-1 DNA in breast milk samples.

MATERIALS AND METHODS

Specimens A total of 243 breast milk samples (Okinawa, 33; Yamaguchi, 20; Kochi, 15; Okayama, 20; Hyogo, 20; Wakayama, 15; Kyoto, 20; Gifu, 20; Fukui, 20; Tokyo, 20; Sendai, 20; Hokkaido, 20) were collected between 2004 and 2010 and archived in the Kyoto University Human Specimen Bank. Written informed consent was obtained from all of the participants. The bank project was reviewed[12] and approved by the Ethics Committee of the Kyoto University Graduate School of Medicine on 14 November 2003 (E25).

PA The screening test was performed using the 243 breast milk and the commercially available SERODIA HTLV-1 test

* To whom correspondence should be addressed. e-mail: matsubara@daiichi-cps.ac.jp

kit (Fujirebio Inc., Tokyo, Japan) for *in vitro* diagnosis.[13] The kit includes gelatin particles that agglutinate in the presence of HTLV-1 antibody in human serum or plasma. The test samples (25 μL) and the positive control serum were prepared by 2-fold dilution up to 1 : 518. After an equal volume of sensitized beads was added, the reactions were visually interpreted in duplicate. The agglutination patterns were interpreted according to the following criteria for an antibody titer of 1/16: particles concentrated in the shape of a button with a smooth round outer margin–negative (−); particles concentrated in the shape of a compact ring with a smooth round outer margin–inconclusive (±); peripheral agglutination of the particles in a definite large ring with a rough multiform outer margin–positive (+); and a film of agglutinated particles spread out uniformly on the bottom of the well–positive (++).

LIA The PA-positive breast milk was assayed for the presence of HTLV-1 antibodies using INNO-LIA™ HTLV I/II Score assays (Innogenetics N.V., Belgium), which was originally designed for testing with serum or plasma. Milk samples (100 μL) were incubated in troughs containing LIA strips at a room temperature (RT, 25°C) overnight for 16 h. This incubation was followed by three washing steps with washing buffer before the addition of an alkaline phosphatase anti-human immunoglobulin conjugate. The samples were then incubated for 30 min at RT. Three washing steps were again performed, followed by incubation with the chromogen 5-bromo-4-chloro-3-indolyl phosphate/nitroblue tetrazolium for 30 min at RT.

PCR The presence of HTLV-I proviral DNA in breast milk was investigated by PCR. The HTLV-1 proviral DNA in test samples was extracted with a QIAamp DNA Blood Mini Kit (Qiagen, Germany). Among the 4 types of primers (*gag*, *env*, pX1, pX2) for the HTLV-1 genome, we selected pX1(+), 5′-CCCACTTCCCAGGGTTTGGACAGAG-3′, and pX1′(−), 5′-CTGTAGAGCTGAGCCGATAACGCG-3′, which had the highest sensitivities.[14,15] The PCR reaction mixture (50 μL) contained 10 nmol deoxynucleotide triphosphate (dNTP), 2.5 U

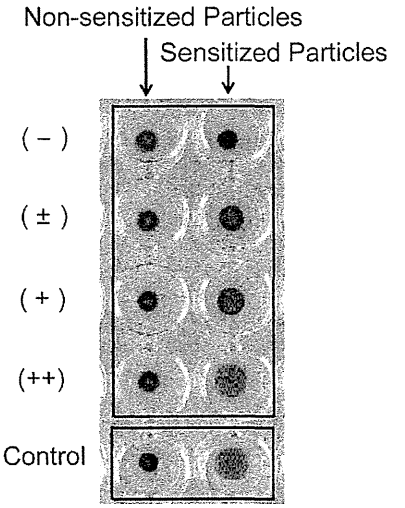

Fig. 1. Agglutination Reactions of Milk Samples with Sensitized Particles

Milk samples were diluted 1 : 16 and reacted with sensitized particles (right side) and non-sensitized particles (left side). Anti-HTLV-I-positive serum was used as a control.

Table 1. Screening Assay for Antibodies to HTLV-1 in Breast Milk Samples Using PA and LIA

No.	Sampling area	Year collected	Age	PA		LIA				Result
				ID[a)]	Titer	p19 I/II	p24 I/II	gp46 I/II	gp21 I/II	
1	Okinawa	2004	26	++	128	—	—	—	—	−
2	Okinawa	2004	25	++	64	—	—	—	—	−
3	Okinawa	2004	26	+	32	—	—	—	—	−
4	Okinawa	2005	31	±	—	—	—	—	—	−
5	Okinawa	2005	35	+	64	—	—	—	—	−
6	Okinawa	2005	29	±	—	—	—	—	—	−
7	Okinawa	2005	29	++	64	—	—	—	—	−
8	Takarazuka	2008	28	±	—	—	—	—	—	−
9	Takarazuka	2008	32	+	32	—	—	+/−	—	−
10	Takarazuka	2009	29	±	—	—	—	—	—	−
11	Sendai	2009	33	++	128	—	—	—	—	−
12	Sendai	2009	30	+	64	—	—	—	—	−
13	Sendai	2009	31	+	64	1+	—	+/−−	1+	+
14	Hokkaido	2005	31	++	64	—	—	—	+/−	±
15	Hokkaido	2005	29	+	32	—	—	—	—	−
16	Hokkaido	2005	33	++	32	+/−	—	—	+/−−	−
17	Hokkaido	2005	28	++	32	—	—	—	—	−
18	Hokkaido	2005	33	++	64	—	—	—	—	−
19	Hokkaido	2005	40	++	64	—	—	—	—	−
20	Hokkaido	2005	30	++	32	—	—	—	—	
21	Hokkaido	2005	35	+	64	—	—	—	+/−−	±
	Negative control			−	−	—	—	—	—	−
	Positive control			++	512	2+	2+	2+	1+	+

a) Evaluated by PA using a 1 : 16 dilution.

Taq polymerase, 10×Ex Taq buffer, 25 pmol of each primer, and adequate sample DNA (1 ng). The amplification was carried with 35 cycles of 5 min of denaturation at 95°C, 2 min of annealing at 68°C, and 2 min of elongation at 72°C. The presence of a 203-bp band was visually compared with that for the positive control DNA from HTLV-1-positive monocytes.

RESULTS AND DISCUSSION

PA The agglutination of breast milk with sensitized beads occurred up to the 6th dilution (1 : 128 titer), whereas the agglutination for the positive control was observed up to the 9th dilution. This finding indicates that the concentration of HTLV-1 antibody in breast milk is one order of magnitude lower than that in the control serum.

At a 1/16 dilution of the test samples, we screened a total of 243 breast milk samples for agglutination reactions. Among the 243 samples, 222 samples were negative (−), 4 samples were deferred, and 17 samples were positive. Figure 1 shows images for reactions classified as (−), (±), (+) and (++).

The results from 21 breast milk samples are shown in Table 1, with the titer of the anti-HTLV-1 antibody ranging from 1/32 to 1/128 (mean, 1/64) for milk samples (n=17) and from 1/256 to 1/1024 for the positive control (n=3). The reaction between each milk sample and non-sensitized particles (1/8 final dilution) was negative. The analysis of the repeatability of the titers (1/64 dilution) for positive milks sample (n=5) revealed a relative standard deviation of less than 10%.

It has been shown that PA can be used not only for the testing of anti-HTLV-1 antibodies but also for screening for ATL and HTLV-1-associated myelopathy.[5,10] In donor screening, the PA method was capable of almost 100% detection for more than 3600 donors in the early stages of infection.[9] The PA kit was designed for the testing of serum or plasma, and the present study is the first to use this PA kit to screen breast milk for infection.

LIA LIA was performed on the 21 samples that positive or deferred in the PA test (Table 1). The presence of the *gag* (p19 I/II) and *env* (gp21 I/II) bands characteristic of HTLV-1 was positive for one sample, indeterminate for two samples, and negative for the other samples. Although the anti-HTLV immunoglobulin G (IgG) antibody titer of the positive control serum was greater than 1 : 100,[16] we could not detect IgG and IgM antibodies against HTLV antigens using ten-fold dilutions of the milk samples. Therefore, this method should be improved by adding a step in which the antibody in the breast milk is further concentrated.

PCR The results of the PCR tests showed that the pX1 bands were not detected in any of the 21 samples, most likely because the amount of provirus DNA was below the detection threshold (16–42 ng of DNA from HTLV-1-positive monocytes) for T-lymphocyte DNA extraction.[17] Kinoshita *et al.* demonstrated the presence of the HTLV-1 antigen in breast milk samples from three sero-positive mothers using the indirect IF method.[11] They found the HTLV antigen in only 3 out of 22 milk samples. We failed to obtain a sufficient number of lymphocytes to allow the detection of the HTLV antigen after culturing the LIA-positive sample whose leukocytes could be counted (100/μL). Bacteria or lipids in breast milk can disrupt the extraction of proviral DNA.

Regional Detection Frequency Table 1 shows the regions corresponding to the 21 samples (Okinawa 7/33, Hyogo 3/20, Miyagi 3/20, Hokkaido 8/20) that are positive by PA among the 243 samples tested in this study. The high PA-positive rate (7/33) for the HTLV-1 antibody in breast milk from Okinawa may be associated with the higher infection rate in the Kyushu region of southern Japan.[18,19] The samples from Hokkaido (Hidaka area) used in this study also exhibited a higher positive rate (8/20) in the PA assay. This area has been reported to be epidemic area in an epidemiological survey.[20] High HTLV-1 infection rates have also been reported in developing countries, where it may be difficult to collect blood samples for testing. As breast milk can be collected non-invasively and prepared anytime with freeze-dried products, PA would be a useful method for the simple and primary screening of breast milk samples, even in the field.

In conclusion, the PA method can be applied to breast milk to screen for anti-HTLV-1 antibodies. One milk sample was confirmed to be positive by the LIA method, and two were found to be indeterminate. A more sensitive PCR method is needed to confirm the presence of HTLV-1 proviral DNA in the LIA-positive samples.

Acknowledgments The authors thank Dr. Yasuko Sagara for critical suggestions and for her kind gift of the HTLV-1-positive monocytes for use as a positive control for the PCR. This study was supported in part by Grants-in-Aid for Health Sciences Research from the Ministry of Health, Labour and Welfare of Japan (H21-Food-003) and by Special Coordination Funds for Promoting Science and Technology (No. 1300001) sponsored by the Japan Science and Technology Agency.

REFERENCES

1) Yamaguchi K, Watanabe T. Human T lymphotropic virus type-I and adult T-cell leukemia in Japan. *Int. J. Hematol.*, **76** (Suppl. 2), 240–245 (2002).
2) Mylonas I, Brüning A, Kainer F, Friese K. HTLV infection and its implication in gynaecology and obstetrics. *Arch. Gynecol. Obstet.*, **282**, 493–501 (2010).
3) Iwanaga M, Watanabe T, Utsunomiya A, Okayama A, Uchimaru K, Koh KR, Ogata M, Kikuchi H, Sagara Y, Uozumi K, Mochizuki M, Tsukasaki K, Saburi Y, Yamamura M, Tanaka J, Moriuchi Y, Hino S, Kamihira S, Yamaguchi K; Joint Study on Predisposing Factors of ATL Development investigators. Human T-cell leukemia virus type I (HTLV-1) proviral load and disease progression in asymptomatic HTLV-1 carriers: a nationwide prospective study in Japan. *Blood*, **116**, 1211–1219 (2010).
4) Ureta-Vidal A, Angelin-Duclos C, Tortevoye P, Murphy E, Lepère JF, Buigues RP, Jolly N, Joubert M, Carles G, Pouliquen JF, de Thé G, Moreau JP, Gessain A. Mother-to-child transmission of human T-cell-leukemia/lymphoma virus type I: implication of high antiviral antibody titer and high proviral load in carrier mothers. *Int. J. Cancer*, **82**, 832–836 (1999).
5) Sonoda T. [Present status of HTLV-I infections in developing countries and the countermeasures]. *Uirusu*, **43**, 93–100 (1993).
6) Proietti FA, Carneiro-Proietti ABF, Catalan-Soares BC, Murphy EL. Global epidemiology of HTLV-I infection and associated diseases. *Oncogene*, **24**, 6058–6068 (2005).
7) Yamaguchi K, Yonemura Y, Okabe H, Takahama Y, Nagai S, Yamaguchi H, Hirai K. Detection of anti-human T-lymphotropic virus type I antibody in whole blood by a novel counting immunoassay. *Clin. Chem.*, **49**, 275–280 (2003).
8) Yamashita N, Maeda M, Tani Y, Shibata H, Yamashita S, Hayashi

N, Matsumoto K. Evaluation of the Taqman polymerase chain reaction method for detection of human T cell lymphotropic virus type I. *Jpn. J. Trans. Med.*, **45**, 366–372 (1999).
9) Li HC, Biggar RJ, Miley WJ, Maloney EM, Cranston B, Hanchard B, Hisada M. Provirus load in breast milk and risk of mother-to-child transmission of human T lymphotropic virus type I. *J. Infect. Dis.*, **190**, 1275–1278 (2004).
10) Matsumoto C, Shiozawa R, Mitsunaga S, Ichikawa A, Ishiwatari R, Uchida S, Nakajima K, Tadokoro K, Juji T. High-throughput HTLV-1 proviral DNA detection system using a nucleic acid extraction robot and real-time PCR detection. *Jpn. J. Trans. Med.*, **47**, 378–383 (2001).
11) Kinoshita K, Hino S, Amagasaki T, Ikeda S, Yamada Y, Suzuyama J, Momita S, Toriya K, Kamihira S, Ichimaru M. Demonstration of adult T-cell leukemia virus antigen in milk from three seropositive mothers. *Jpn. J. Cancer Res.*, **75**, 103–105 (1984).
12) Koizumi A, Harada KH, Inoue K, Hitomi T, Yang H-R, Moon C-S, Wang P, Hung NN, Watanabe T, Shimbo S, Ikeda M. Past, present, and future of environmental specimen banks. *Environ. Health Prev. Med.*, **14**, 307–318 (2009).
13) Fujirebio Inc. "SERODIA® HTLV-I.": ‹http://www.fujirebio.co.jp/english/product/serodia.html#03›, cited 2011.
14) Burmeister T, Schwartz S, Thiel E. A PCR primer system for detecting oncoretroviruses based on conserved DNA sequence motifs of animal retroviruses and its application to human leukaemias and lymphomas. *J. Gen. Virol.*, **82**, 2205–2213 (2001).
15) Poiesz BJ, Ruscetti FW, Gazdar AF, Bunn PA, Minna JD, Gallo RC. Detection and isolation of type C retrovirus particles from fresh and cultured lymphocytes of a patient with cutaneous T-cell lymphoma. *Proc. Natl. Acad. Sci. U.S.A.*, **77**, 7415–7419 (1980).
16) Zrein M, Louwagie J, Boeykens H, Govers L, Hendrickx G, Bosman F, Sablon E, Demarquilly C, Boniface M, Saman E. Assessment of a new immunoassay for serological confirmation and discrimination of human T-cell lymphotropic virus infections. *Clin. Diagn. Lab. Immunol.*, **5**, 45–49 (1998).
17) Umeki K, Hisada M, Maloney EM, Hanchard B, Okayama A. Proviral loads and clonal expansion of HTLV-1-infected cells following vertical transmission: a 10-year follow-up of children in Jamaica. *Intervirology*, **52**, 115–122 (2009).
18) Zane L, Sibon D, Mortreux F, Wattel E. Clonal expansion of HTLV-1 infected cells depends on the CD4 *versus* CD8 phenotype. *Front. Biosci.*, **14**, 3935–3941 (2009).
19) Takeda S, Maeda M, Morikawa S, Taniguchi Y, Yasunaga J, Nosaka K, Tanaka Y, Matsuoka M. Genetic and epigenetic inactivation of tax gene in adult T-cell leukemia cells. *Int. J. Cancer*, **109**, 559–567 (2004).
20) Kwon KW, Yano M, Sekiguchi S, Iwanaga M, Fujiwara S, Oikawa O, Sugiura M, Imai S, Osato T. Prevalence of human T-cell leukemia virus type 1 (HTLV-I) in general inhabitants in non-adult T-cell leukemia (ATL)-endemic Hokkaido, Japan. *In Vivo*, **8**, 1011–1014 (1994).

Environ Health Prev Med (2012) 17:292–298
DOI 10.1007/s12199-011-0251-9

REGULAR ARTICLE

Preliminary assessment of ecological exposure of adult residents in Fukushima Prefecture to radioactive cesium through ingestion and inhalation

Akio Koizumi · Kouji H. Harada · Tamon Niisoe · Ayumu Adachi · Yukiko Fujii · Toshiaki Hitomi · Hatasu Kobayashi · Yasuhiko Wada · Takao Watanabe · Hirohiko Ishikawa

Received: 21 October 2011 / Accepted: 23 October 2011 / Published online: 10 November 2011

Abstract

Objective This study aims to estimate the ecological exposure of adult residents of Fukushima Prefecture to ^{134}cesium (Cs) and ^{137}Cs through ingestion and inhalation between July 2 and July 8, 2011.

Methods Fifty-five sets of meals with tap water, each representing one person's daily intake, were purchased in local towns in Fukushima Prefecture. Locally produced cow's milk (21 samples) and vegetables (43 samples) were also purchased. In parallel, air sampling was conducted at 12 different sites using a high-volume sampler. Nineteen sets of control meals were collected in Kyoto in July 2011. ^{134}Cs and ^{137}Cs levels in the samples were measured using a germanium detector.

Results Radioactivity was detected in 36 of the 55 sample meals from Fukushima, compared with one of 19 controls from Kyoto. The median estimated dose level (μSv/year) was 3.0, ranging from not detectable to 83.1. None of the cow's milk (21) or vegetable (49) samples showed levels of contamination above the current recommended limits (Bq/kg) of 200 for milk and 500 for vegetables. The total effective dose levels by inhalation were estimated to be <3 μSv/year at nine locations, but samples at three other locations close to the edge of the 20-km radius from the crippled nuclear power plant showed higher levels of contamination (μSv/year): 14.7 at Iitate, 76.9 at Namie, and 27.7 at Katsurao.

Conclusions Levels of exposure to ^{134}Cs and ^{137}Cs in Fukushima by ingestion and inhalation are discernible, but generally within recommended limits.

Keywords ^{134}Cs · ^{137}Cs · Exposure assessment · Fukushima Daiichi nuclear power plant accident · Ingestion · Inhalation

Electronic supplementary material The online version of this article (doi:10.1007/s12199-011-0251-9) contains supplementary material, which is available to authorized users.

A. Koizumi (✉) · K. H. Harada · T. Niisoe · A. Adachi · Y. Fujii · T. Hitomi · H. Kobayashi
Department of Health and Environmental Sciences, Kyoto University Graduate School of Medicine, Kyoto 606-8501, Japan
e-mail: koizumi.akio.5v@kyoto-u.ac.jp

Y. Wada
Department of Lifestyle Design, Faculty of Human Life and Environmental Science, University of Kochi, Kochi 780-8515, Japan

T. Watanabe
Tohoku Bunkyo College, Yamagata 990-2361, Japan

H. Ishikawa (✉)
Severe Storm and Atmospheric Environment Section, Research Division of Atmospheric and Hydrospheric Disaster Division, Disaster Prevention Research Institute, Kyoto University, Uji 611-0011, Japan
e-mail: ishikawa@storm.dpri.kyoto-u.ac.jp

Introduction

Following the Tohoku earthquake and tsunami on March 11, 2011, the Fukushima Daiichi nuclear power plant exploded on March 15, 2011, releasing massive amounts of radionuclides, including iodine, cesium (Cs), strontium, and plutonium into the northern part of Japan and the Pacific Ocean, being the second largest nuclear accident, after the Chernobyl disaster [1, 2]. The total amount of ^{137}Cs released into the environment by the Fukushima Daiichi nuclear plant from March 11 to April 15

(1.3×10^{16} Bq) [3] has been estimated to be 10% of that emitted by the Chernobyl disaster in 1986 [1, 2].

Residents living within a 20-km radius of the nuclear power plant were evacuated soon after the disaster, but people in Fukushima Prefecture have continued to live outside this evacuation zone. Although the direct threat from the radioactive plume is over, it is important to continuously assess the exposure doses due to deposited radioactivity. Contamination with ^{137}Cs has been reported in residential areas in Fukushima Prefecture [4], and the internal doses resulting from inhalation of resuspended deposits [5] and ingestion of contaminated foods need to be monitored.

Residents in particular, but also people in remote areas, are seriously concerned about their levels of internal exposure to radionuclides through ingestion of contaminated food and drink. The ingested dose should be evaluated on the basis of the level of radioactivity contained in complete meals consumed (Bq/day/person), rather than on the radioactive content of an individual item (Bq/kg).

To evaluate potential post-accident internal doses, we conducted a field survey in July 2011, focusing on estimated exposures of adult residents of Fukushima Prefecture to ^{134}Cs and ^{137}Cs through ingestion and inhalation.

Materials and methods

Field survey

We tested whole-day meals, vegetables from local food venders, tap water, and air samples from cities at various distances from the nuclear power plant between July 2 and July 8, 2011 (Fig. 1). In the cities denoted as "M" and "V" in Fig. 1, we purchased whole-day meals and vegetables from local food venders, respectively. Tap water was also collected in the same towns or cities. In the cities denoted by "A," we conducted air sampling using a high-volume sampler (HV-1000F; Sibata, Saitama, Japan) and soil sampling (mixed soil samples from depth of 0–5 cm). We also collected continuous air samples at a fixed point in Fukushima City using a low-volume sampler (SL-30; Sibata, Saitama, Japan) with an eight-stage Andersen cascade impactor sampler (AN-200; Tokyo Dylec Co., Tokyo, Japan).

Food collection and processing for radioactivity determinations

Five male researchers (aged 32–68 years) visited one of the most popular local grocery stores in each city or town and purchased several sets of whole-day meals, according to their personal preferences, as reported previously [6]. A set of whole-day meals comprised prepackaged breakfast, lunch, and dinner, as well as desserts, snacks, and

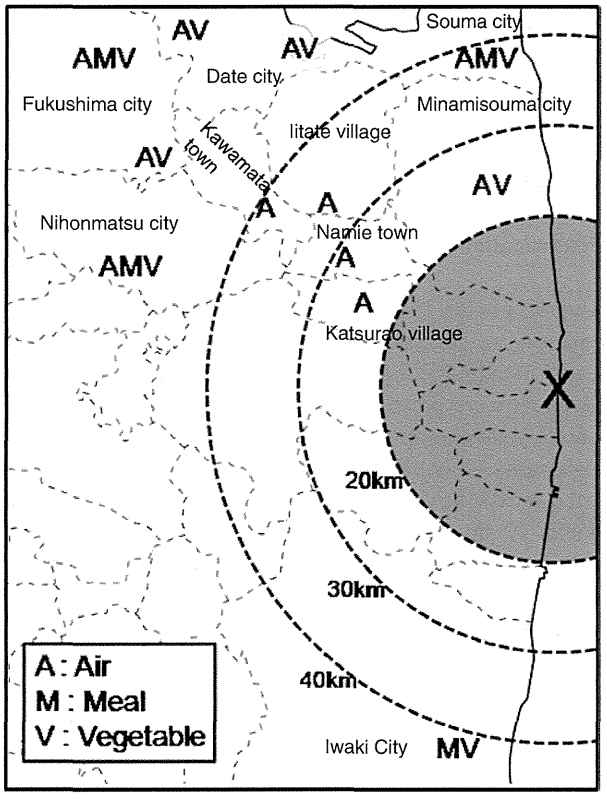

Fig. 1 Geographical locations of the field study areas. "A" represents sites where air sampling was conducted. "M" represents grocery stores where meals were purchased. Tap water (12 L) was collected in the same towns where meals were purchased. "V" represents commercial vender where vegetables were purchased. "X" represents the Fukushima Daiichi nuclear power plant. The *symbols* approximately represent actual geographical positions

beverages. A total of 12 L geographically matched tap water per town was donated by residents of the towns where the grocery stores were located. Locally produced vegetables and cow's milk were also purchased in the same towns. All items were transported daily to Kyoto University at 4°C for processing and analysis.

Daily whole-day meal sets were homogenized with locally collected tap water (approximately 1 L), together with desserts and snacks. The final volumes were recorded, and approximately 1 L of each homogenate was processed for freeze-drying. Vegetables and cow's milk were also freeze-dried. Control meals consisted of whole-day meals collected by 19 females using the food duplicate method, as previously reported [6]. Control meals were collected in July 2011 in Uji, Kyoto, which is located from 540 km to the southwest of the Fukushima nuclear power plant.

Air sampling and determination of radioactivities

A high-volume air sampler was used to collect dust in the air on a quartz membrane filter. A minimum of 50 m^3 was

inspired at all sampling sites at a height of 1.5 m above ground. An Andersen low-volume sampler was used to collect dust of various aerodynamic diameters to estimate the respirable portion of dust in Fukushima Prefecture. This sampler was fixed at a sampling site in Fukushima City. Dust samples were weighed, and their radioactivities were measured.

Determination of ^{137}Cs and ^{134}Cs

Aliquots of 100–200 g from each sample of food and cow's milk (dry weight), and soil (fresh weight) were weighed and sealed in cylindrical plastic containers. Filters from aerosol sampling were pressed into small cylindrical plastic containers. Radiometric determinations were performed using a high-purity, low-background, high-resolution germanium detector (0.7 keV). The detector was protected by a lead shield, 10 cm thick internally, covered with 0.5 mm electrolytic copper. A multichannel analyzer (4,096 channels, range 0–3,000 keV, MCA8000; Princeton Gamma Technologies, NJ, USA) was used for gamma-spectrum acquisition and processing. Characteristic gamma-ray energies were monitored to identify and quantify the radionuclides (^{134}Cs 604.7 and 795.9 keV, ^{137}Cs 661.7 keV). The detector was calibrated using a gamma-ray reference source from the Japan Radioisotope Association (Tokyo, Japan). The gamma spectrum of each sample was measured for >20,000 s for food and dust samples and for >2,000 s for soil samples. The lower limits of detection were 0.05 Bq/kg, 0.2 Bq/kg, 0.2 Bq/kg, 0.2 mBq/m^3, and 1 Bq/kg for food, vegetable, milk, dust, and soil samples, respectively. All samples were assumed to be in radioactive equilibrium. All activities were corrected to March 15, 2011 using physical half-lives (^{134}Cs 2.06 years, ^{137}Cs 30.1 years).

Effective dose coefficients for exposures by ingestion and inhalation

Radioactivities were converted into effective doses using effective dose coefficients of 0.019 μSv/Bq for ^{134}Cs and 0.013 μSv/Bq for ^{137}Cs by ingestion, respectively [7]. For inhalation, we assumed that a standard adult resident inhaled 20 m^3 air per day and used the effective dose coefficients of 0.02 μSv/Bq for ^{134}Cs and 0.039 μSv/Bq for ^{137}Cs for inhalation [7]. For the two routes of exposure, we postulated conservatively that all the radionuclides were retained in the body or in the lung, with no elimination.

Results and discussion

A total of 74 sets of whole-day meals were collected and analyzed. Their menus and components are presented in

Table 1 Dietary intake of radioactive cesium in Fukushima Prefecture

Sampling site	*n*		Food volume (g/day)	Water content (%)	Daily intake (Bq/day)		Estimated dose (μSv/year)
					^{134}Cs	^{137}Cs	
Fukushima total	55	*n* > MDL (%)	–	–	36 (65.5)	35 (63.6)	
		Median (range)	2,053 (1,100–3,145)	80.8 (73.3–97.6)	0.2 (ND–7.2)	0.3 (ND–7.0)	3.0 (ND–83.1)
		Mean ± SD	2,178 ± 400	81.9 ± 4.5	0.5 ± 1.1	0.6 ± 1.0	6.4 ± 12.5
Iwaki	10	*n* > MDL (%)	–	–	9 (90.0)	9 (90.0)	
		Median (range)	2,241 (1,879–2,690)	82.1 (76.8–86.1)	0.4 (ND–2.5)	0.7 (ND–1.6)	6.5 (ND–24.7)
		Mean ± SD	2,238 ± 272	81.5 ± 3.3	0.7 ± 0.8	0.7 ± 0.5	8.6 ± 7.8
Souma	10	*n* > MDL (%)	–	–	7 (70.0)	8 (80.0)	
		Median (range)	2,451 (2,044–2,795)	80.5 (73.3–87.1)	0.6 (ND–7.2)	0.9 (ND–7.0)	8.2 (ND–83.1)
		Mean ± SD	2,395 ± 293	80.1 ± 4.2	1.4 ± 2.2	1.6 ± 2.2	17.4 ± 25.3
Nihonmatsu	10	*n* > MDL (%)	–	–	5 (50.0)	4 (40.0)	
		Median (range)	2,611 (1,964–3,145)	79.4 (75.1–82.6)	0.1 (ND–0.9)	ND (ND–0.9)	1.7 (ND–10.4)
		Mean ± SD	2,529 ± 423	78.9 ± 2.3	0.3 ± 0.4	0.2 ± 0.3	2.9 ± 3.6
Fukushima	25	*n* > MDL (%)	–	–	15 (60.0)	14 (56.0)	
		Median (range)	1,954 (1,100–3,051)	83.7 (77.9–97.6)	0.1 (ND–0.8)	0.2 (ND–1.3)	1.3 (ND–11.3)
		Mean ± SD	1,927 ± 308	84.1 ± 4.8	0.2 ± 0.2	0.2 ± 0.3	2.6 ± 3.1
Kyoto (Uji)	19	*n* > MDL (%)	–	–	1 (5.3)	1 (5.3)	–
		Maximum	–	–	0.4	0.5	5.3
		Mean ± SD	2,955 ± 652	87.2 ± 2.5	–	–	–

Estimated dose is the total for doses attributable to exposure to ^{134}Cs and ^{137}Cs. The effective dose coefficients for ^{134}Cs and ^{137}Cs by oral route were 0.019 and 0.013 μSv/Bq, respectively

MDL method detection limit, *ND* less than MDL

Table 2 Radioactive cesium in local commercial products purchased in Fukushima Prefecture

Sampling site	*n*		Weight (g)	Radioactivity (Bq/kg)			Recommended standard[a] (Bq/kg)
				^{134}Cs	^{137}Cs	Total	
Milk							200
Fukushima total	21	*n* > MDL (%)	–	20 (95.2)	19 (90.5)	–	
		Median (range)	–	1.8 (ND–4.9)	1.9 (ND–5.5)	4.1 (ND–10.1)	
		Mean ± SD	985 ± 119	2.1 ± 1.7	2.4 ± 1.9	4.5 ± 3.6	
Iwaki	3	*n* > MDL (%)	–	3 (100.0)	3 (100)		
		Median (range)	–	0.9 (0.6–1.2)	1.2 (1.1–1.3)	2.0 (1.9–2.3)	
		Mean ± SD	752 ± 202	0.9 ± 0.3	1.2 ± 1.1	2.1 ± 0.2	
Souma	6	*n* > MDL (%)	–	6 (100.0)	6 (100.0)	–	
		Median (range)	–	3.1 (1.4–3.8)	3.1 (1.9–4.4)	6.1 (3.3–8.2)	
		Mean ± SD	1,019 ± 29	2.8 ± 1.0	3.1 ± 1.0	5.9 ± 1.9	
Nihonmatsu	3	*n* > MDL (%)	–	3 (100.0)	1 (33.3)		
		Median (range)	–	0.2 (0.2–1.3)	ND (ND–1.1)	0.2 (0.2–2.4)	
		Mean ± SD	1,047 ± 15	0.5 ± 0.7	0.4 ± 0.6	0.9 ± 1.3	
Fukushima	9	*n* > MDL (%)	–	8 (88.9)	8 (88.9)	–	
		Median (range)	–	3.4 (ND–4.9)	3.9 (ND–5.5)	7.3 (0.2–10.1)	
		Mean ± SD	1,021 ± 18	2.6 ± 2.0	2.3 ± 4.4	5.6 ± 4.4	
Kyoto (Uji)	3	*n* > MDL (%)	–	1 (33.3)	1 (33.3)	–	
		Median (range)	–	ND (ND–0.7)	ND (ND–0.7)	ND (ND–1.4)	
		Mean ± SD	1,037 ± 21	0.2 ± 0.4	0.2 ± 0.4	0.5 ± 0.8	

	Weight (g)	Radioactivity (Bq/kg weight)			Recommended standard[a] (Bq/kg)
		^{134}Cs	^{137}Cs	Total	
Vegetable/fruit					500
Kyoto (Uji)					
Spinach	1,249	ND	ND	ND	
Japanese mustard spinach	3,044	ND	ND	ND	
Fukushima (n = 43)					
Date					
Japanese mustard spinach	1,828	2.6	2.2	4.8	
Spinach	1,677	0.2	0.3	0.5	
New Zealand spinach	1,097	29.9	32.7	62.6	
Ceylon spinach	826	2.1	3.1	5.2	
Cucumber	1,643	3.4	4.5	7.9	
Welsh onion	1,770	3.3	2.8	6.1	
Kawamata					
Mizuna	504	5.9	7.7	13.7	
Shiitake	1,012	140.4	164.2	304.6	
Ceylon spinach	503	4.4	3.0	7.4	
Cucumber	1,007	1.3	1.6	2.8	
Broccoli	831	6.4	6.6	12.9	
Chinese chives	704	7.2	4.5	11.7	
Partially dried Japanese persimmon	332	1.8	1.7	3.5	
Welsh onion	1,455	5.7	6.6	12.3	
Fukushima					
Chinese chives	436	1.9	2.0	3.9	
Cucumber	493	2.9	3.9	6.8	

Table 2 continued

	Weight (g)	Radioactivity (Bq/kg weight)			Recommended standard[a] (Bq/kg)
		^{134}Cs	^{137}Cs	Total	
Iwaki					
Spinach	1,903	0.5	0.9	1.4	
Snap bean	860	3.5	3.6	7.1	
Shiitake	89	ND	ND	ND	
Green onion	571	7.3	8.5	15.8	
Chinese chives	615	2.8	3.5	6.3	
Broccoli	1,479	0.9	1.1	2.0	
Ceylon spinach	1,079	1.5	2.6	4.0	
Garlic	691	0.8	0.5	1.3	
Souma					
Welsh onion	1,543	4.1	2.6	6.7	
Peach	794	9.3	7.9	17.2	
Cherry	244	29.3	37.3	66.6	
Broad beans	418	4.9	6.0	10.9	
Onion (large)	835	0.5	0.6	1.1	
Onion (small)	430	9.1	9.2	18.3	
Red onion (large)	589	3.3	5.0	8.3	
Red onion (small)	524	9.6	11.6	21.3	
Garlic	256	9.4	7.2	16.6	
Potato	1,258	1.0	0.8	1.8	
Minamisouma					
Carrot	1,271	1.4	2.1	3.5	
Shiitake	417	127.1	154.7	281.8	
Bell pepper	502	ND	ND	ND	
Nihonmatsu					
Asparagus	637	1.3	1.5	2.8	
Bell pepper	390	12.0	10.7	22.7	
Ceylon spinach	1,533	1.7	3.2	4.9	
Cucumber	2,064	3.6	4.3	7.9	
Welsh onion	1,309	5.4	5.0	10.5	
Cherry	352	24.5	28.5	52.9	

MDL method detection limit, *ND* less than MDL

[a] Recommended by Ministry of Health, Labor, and Welfare of Japan [8]

Table S1. Radioactivity per daily intake (Bq/day) is also summarized in Table 1. ^{134}Cs or ^{137}Cs was detected in 36 of 55 whole-day meal samples from Fukushima Prefecture, compared with only one of 19 from Kyoto. The estimated median dose levels was 3.0 μSv/year, ranging from not detectable (ND) to 83.1 μSv/year in Fukushima, while the maximum dose level in Kyoto was 5.3 μSv/year.

The levels of ^{134}Cs and ^{137}Cs in cow's milk and vegetables were also determined (Table 2). The median total activity in milk from Fukushima Prefecture was 4.1 Bq/kg, ranging from ND to 10.1, which was an order of magnitude lower than the recommended limit set by the Ministry of Health, Labor, and Welfare of Japan [8]. Trace radioactivity was detected in only one sample from Kyoto. No vegetables in Fukushima Prefecture exceeded 100 Bq/kg, except for shiitake mushrooms (*Lentinula edodes*), which contained relatively high levels of radioactivity, up to 60% of the recommended limit (Table 2). Radioactivities in shiitake at Kawamata or Minamisouma were larger than at Iwaki, indicating that a radioactive plume was transferred by northeasterly winds from the nuclear plant. No radioactivity was detected in vegetables from Kyoto. These results indicate that the levels of radioactive Cs ingested were well below the recommended limits [8] in various towns in Fukushima Prefecture, except in the case of shiitake.

Table 3 Particle size distribution and respiratory deposition estimate for radioactive cesium in Fukushima Prefecture

Sampling site		Date (2011)	Andersen low-volume sampler, 224 m^3			
			Fraction (μm)	Dust amount (mg)	Radioactivity (mBq/m^3-air)	
					^{134}Cs	^{137}Cs
Fukushima	37°45′42″N 140°28′18″E	7/2–7/8	100–11.4	0.7	0.4	0.3
			11.4–7.4	1.1	0.3	0.3
			7.4–4.9	1	1.0	0.4
			4.9–3.3	0.9	0.5	0.6
			3.3–2.2	0.6	0.3	0.2
			2.2–1.1	0.8	0.3	0.2
			1.1–0.7	1.3	0.8	0.4
			0.7–0.46	1.3	1.5	1.1
			<0.46	0.9	1.5	1.3
		Total		8.6	6.5	4.7
		Respirable	<4.9	5.8	4.8	3.8

Sampling site		Date (2011) (weather)	High-volume air sampler							Ambient dose rate	Radioactivity in soil (Bq/kg)		
			Air volume sampled (m^3)	Dust amount (mg)	Radioactivity in air (mBq/m^3-air)		Estimated dose[a] (μSv/year)						
					^{134}Cs	^{137}Cs	^{134}Cs	^{137}Cs	Total	(μSv/h)	^{134}Cs	^{137}Cs	*n*
Fukushima	37°45′42″N 140°28′18″E	2011/7/2 (F)	473	6.8	1.9	3.0	0.3	0.8	1.1	1.2	NA	NA	
Date	37°47′10″N 140°33′26″E	2011/7/3 (CL)	94	3.5	7.9	6.4	1.1	1.8	3.0	0.9	3,232 ± 2,666	3,855 ± 3,047	5
Fukushima	37°39′26″N 140°32′11″E	2011/7/3 (CL)	83	1.9	4.7	1.5	0.7	0.4	1.1	1.0	2,515 ± 859	3,059 ± 1,077	5
Fukushima	37°45′42″N 140°28′18″E	2011/7/4 (R)	450	8	1.6	1.5	0.2	0.4	0.6	1.2	NA	NA	
Souma	37°46′1″N 140°57′2″E	2011/7/5 (F)	88	0.7	0.6	0.2	0.1	0.1	0.1	0.5	1,710 ± 2,365	2,116 ± 2,976	5
Minami-Souma	37°38′29″N 140°55′30″E	2011/7/5 (F)	84	2.4	0.7	1.1	0.1	0.3	0.4	0.9	1,772 ± 411	2,151 ± 546	5
Souma	37°46′8″N 140°43′1″E	2011/7/5 (F)	84	1.3	1.1	2.3	0.2	0.7	0.8	1.6	1,723 ± 1,792	2,047 ± 2,174	5
Fukushima	37°45′42″N 140°28′18″E	2011/7/5 (F)	220	4	2.9	3.4	0.4	1.0	1.4	1.2	NA	NA	
Nihonmatsu	37°33′21″N 140°27′34″E	2011/7/6 (F)	93	0.1	0.6	0.6	0.1	0.2	0.3	1.2	12,184 ± 12,170	14,202 ± 14,025	5
Nihonmatsu	37°33′21″N 140°30′43″E	2011/7/6 (F)	53	0.3	4.2	7.3	0.6	2.1	2.7	1.9	1,895 ± 674	2,244 ± 755	5
Kawamata	37°36′14″N 140°38′49″E	2011/7/6 (CL)	72	0.4	6.3	6.1	0.9	1.7	2.7	2.0	3,931 ± 4,856	4,741 ± 5,929	5
Fukushima	37°45′42″N 140°28′18″E	2011/7/6 (CL)	246	4	5.3	7.6	0.8	2.2	2.9	1.2	NA	NA	
Fukushima	37°45′42″N 140°28′18″E	2011/7/7 (CL)	259	5.3	1.9	2.5	0.3	0.7	1.0	1.2	NA	NA	
Iitate	37°36′44″N 140°44′52″E	2011/7/7 (CL)	84	1.7	24.6	38.9	3.6	11.1	14.7	9.0	18,531 ± 11,235	23,185 ± 15,664	5
Namie	37°33′38″N 140°45′39″E	2011/7/7 (CL)	84	1.7	148.2	194.2	21.6	55.3	76.9	13.0	13,548 ± 10,469	16,216 ± 12,653	5
Katsurao	37°31′33″N 140°48′21″E	2011/7/7 (CL)	84	1.5	65.0	64.0	9.5	18.2	27.7	10.0	16,332 ± 11,170	16,799 ± 10,058	5

CL cloudy, *F* fine, *R* rainy, *NA* not available

[a] It was assumed that radioactive cesium was in respirable fraction and that a standard human inhales 20 m^3 air

We collected 16 dust samples using the high-volume sampler (Table 3; Fig. 1). Data obtained with the low-flow-volume sampler suggested that a large proportion of the radionuclides from the crippled Fukushima nuclear power plant was in the respirable fraction: 74% (4.8/6.5) of the total ^{134}Cs and 81% (3.8/4.7) of the total ^{137}Cs (Table 3). To estimate the exposure doses for humans, we therefore selected a conservative scenario whereby all ^{134}Cs and ^{137}Cs activities in the dust samples collected using the high-volume sampler were allocated to the respirable fraction (aerodynamic diameter <4.9 μm). The highest dose level of 76.9 μSv/year was recorded in a sample collected at Namie. However, this value was still less than one-tenth of the permissible dose level of 1 mSv/year [8]. The estimated dose levels for ^{137}Cs were significantly correlated with ambient dose rate (μSv/h) ($n = 10$, $r^2 = 0.79$, $p < 0.05$) but not with mean radioactivity levels in soil (Bq/kg) ($n = 11$, $r^2 = 0.32$, $p > 0.05$).

Given that the samples in this study were obtained in early July, about 4 months after the major release of radioactivity, airborne radioactivity was likely to represent resuspended deposited radioactivity, rather than direct transport from the source. Several studies have investigated resuspension from a flat surface [5], but information on resuspension from ecological systems including forests and paddy fields is scant.

We demonstrated the radioactivity levels due to ^{134}Cs and ^{137}Cs in Fukushima Prefecture in July 2011. The maximum total exposure dose through inhalation and ingestion was estimated to be 160 μSv/year (83.1 by ingestion and 76.9 by inhalation) in zones outside a 20-km radius of the crippled Fukushima nuclear power plant.

The amounts of radioactivity in the daily meals consumed by residents of the study regions were well below the regulation limit. However, many food items are now imported globally, such that a high portion of foodstuffs comes from uncontaminated areas. It is possible that the radioactivity in some highly contaminated foodstuffs may be diluted by other "clean" foods. However, the ingested doses estimated in the present study would underestimate the exposure of residents whose daily foods are mostly supplied locally from within the contaminated areas. The conclusions of this study may therefore not be applicable to people in such a situation. Furthermore, the current study only utilized air monitoring in a few, geographically limited areas. All meal samples were obtained from outside a 30-km radius of the nuclear power plant, because no commercial venders were present between 20 and 30 km from the power plant, which had been defined as the planned emergency evacuation zone. In addition to the small number of air samples collected, the survey was conducted in the rainy season when "resuspension" is relatively low. The current study is thus subject to the above limitations and biases. However, the conservative approach adopted in this study maximized the estimated dose levels and would thus partially mitigate the effects of any biases and limitations. In conclusion, the estimated dose levels in residents of Fukushima Prefecture as a result of ingestion and inhalation were much lower than the 1 mSv/year, recognized as a publicly permissible dose [8]. Further studies are needed to perform qualitative risk assessments based on more accurate exposure estimates.

Acknowledgments This study was supported by a Grant-in-Aid for Health Sciences Research from the Ministry of Health, Labor, and Welfare of Japan (H21-Food-003), an urgent collaborative research grant from the Disaster Prevention Research Institute, Kyoto University (23U-01), and Tokyo Kenbikyoin Foundation.

Conflicts of interest The authors declare that there are no conflicts of interest.

References

1. Fukushima radioactive fallout nears Chernobyl levels. Newscientist.com. 2011. http://www.newscientist.com/article/dn20285-fukushima-radioactive-fallout-nears-chernobyl-levels.html. Accessed 24 Apr 2011.
2. Peter Grier. Was Chernobyl really worse than Fukushima? The Christian Science Monitor. 2011. http://www.csmonitor.com/USA/2011/0426/Was-Chernobyl-really-worse-than-Fukushima. Accessed 26 Apr 2011.
3. Chino M, Nakayama H, Nagai H, Terada H, Katata G, Yamazawa H. Preliminary estimation of release amounts of ^{131}I and ^{137}Cs accidentally discharged from the Fukushima Daiichi nuclear power plant into the atmosphere. J Nucl Sci Tech. 2011;48:1129–34.
4. Tsuji M, Kanda H, Kakamu T, Kobayashi D, Miyake M, Hayakawa T, Mori Y, Okochi T, Hazama A, Fukushima T. An assessment of radiation doses at an educational institution 57.8 km away from the Fukushima Daiichi nuclear power plant 1 month after the nuclear accident. Environ Health Prev Med. 2011. doi: 10.1007/s12199-011-0229-7.
5. Ishikawa H. Evaluation of the effect of horizontal diffusion on the long-range atmospheric transport simulation in Chernobyl data. J Appl Meteorol. 1995;34:1653–65.
6. Koizumi A, Harada KH, Inoue K, Hitomi T, Yang HR, Moon CS, Wang P, Hung NN, Watanabe T, Shimbo S, Ikeda M. Past, present, and future of environmental specimen banks. Environ Health Prev Med. 2009;14:307–18.
7. International Commission on Radiological Protection (ICRP). Age-dependent doses to the members of the public from intake of radionuclides—part 5 compilation of ingestion and inhalation coefficients. ICRP Publication 72. Ann ICRP. 1995;26(1).
8. Department of Food Safety, Ministry of Health, Labour and Welfare. Handling of food contaminated by radioactivity (Relating to the accident at the Fukushima Nuclear Power Plant). March 17, 2011. http://www.mhlw.go.jp/stf/houdou/2r9852000001558e-img/2r98520000015apy.pdf and http://www.mhlw.go.jp/stf/houdou/2r9852000001558e-img/2r98520000015av4.pdf

Environmental Science & Technology

Article

pubs.acs.org/est

Analysis of Perfluoroalkyl Carboxylic Acids in Composite Dietary Samples by Gas Chromatography/Mass Spectrometry with Electron Capture Negative Ionization

Yukiko Fujii,[†] Kouji H. Harada,[†] and Akio Koizumi*

Department of Health and Environmental Sciences, Kyoto University Graduate School of Medicine, Yoshida, Kyoto 606-8501, Japan

Supporting Information

ABSTRACT: A gas chromatography–mass spectrometry and electron-capture negative ionization (ECNI) method was developed to quantify perfluorinated carboxylic acids (PFCAs) in composite dietary samples. Benzyl esterification was used for pretreatment before PFCAs analysis. This stabilized the benzyl radical leaving group preferentially, and gave carboxylic anions of the PFCAs with ECNI. The method had a low detection limit (0.3–10 pg g^{-1}) and good recoveries (98–90%) for PFCAs with 8–14 carbon atoms (C8 to C14). The method was applied to 24-h dietary samples from subjects in Japan (Hokkaido, Kyoto, and Okinawa; 1992 to 2007, and 2009), Korea (Seoul; 1994 and 2007), and China (Beijing; 1993 and 2009). The levels of the PFCAs were between 39 and 169 ng day^{-1} in Korea, 58 and 71 ng day^{-1} in China, and 56 and 67 ng day^{-1} in Japan. Between the two sampling years, the total levels of PFCAs (C8 to C14) increased significantly ($p < 0.05$). The interaction between the sampling location in Korea and year was significant ($p < 0.05$).

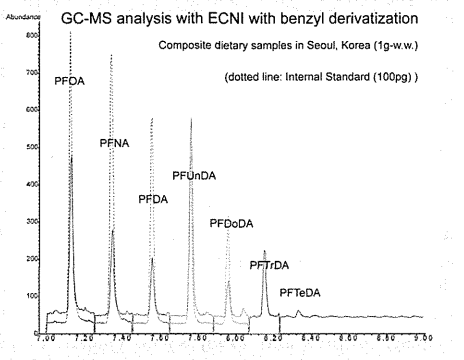

1. INTRODUCTION

Perfluorochemicals such as perfluorooctane sulfonate (PFOS) and perfluorooctanoic acid (PFOA) are environmental contaminants of public health concern because of their persistence and bioaccumulation in the environment. They have been detected in human serum and breast milk samples in many areas.[1] However, the exposure routes are not well characterized. The 3M Company was a major manufacturer of PFOS, but phased out its production in 2002.[2] Since then, concern has shifted from PFOS to PFOA. However, in Japan, perfluorinated carboxylic acid (PFCA) emissions contain perfluorononanoic acid (PFNA) and perfluoroundecanoic acid (PFUnDA) in addition to PFOA. [3] In 2000, 25 and 7 t (1 t = 1000 kg) of PFNA and PFUnDA were emitted, respectively.[3] In an earlier study, we detected PFNA and PFUnDA at concentrations comparable to PFOA in serum samples from Japanese, Korean, and Vietnamese adults.[4] The levels of these chemicals have continued to increase in humans, even after production of PFOS was halted in 2002,[4] but the exposure routes that are contributing to these increases are still unknown.

Although dietary intake is thought to be a major route of exposure for PFCAs,[5] there is little data for long-chain PFCA levels in food items because of analytical difficulties with method development in liquid chromatography and mass spectrometry (LC/MS).[6] Quantitative analyses of PFCAs at low pg g^{-1} concentrations in complex matrices such as food require rigorous and complicated cleanup procedures to eliminate matrix effects.[7] Alternatively, gas chromatography–mass spectrometry (GC/MS) can be used as the matrix suppression effect caused by coeluting material is relatively low compared with LC/MS.[8] Electron-capture negative ionization (ECNI) reportedly improves the detection limits of PFCA anilides,[9] and could be coupled with GC/MS.

The aim of the present study was to develop a simple but sensitive quantification method for PFCAs in foods. GC/MS was coupled with ECNI for PFCAs analysis. ECNI improved the sensitivity for PFCAs benzyl esters compared with electron impact ionization (EI). PFCAs in composite dietary samples were quantified by this method, and historical trends in the dietary intake of PFCAs in three Asian countries were analyzed.

2. MATERIALS AND METHODS

2.1. Chemicals. Acetone (LC-MS grade), sodium carbonate (>99.5%), and distilled water (LC-MS grade) were obtained from Kanto Chemicals (Tokyo, Japan). Benzyl bromide, tetrabutylammonium hydrogen sulfate, 11H-perfluoroundecanoic acid, and methyl tertiary-butyl ether (MTBE, HPLC grade) were purchased from Wako Pure Chemical Industries (Osaka, Japan). A mixture of $^{13}C_2$-labeled perfluorohexanoic acid, $^{13}C_4$-labeled PFOA, $^{13}C_5$-labeled PFNA, $^{13}C_2$-labeled PFDA, $^{13}C_2$-labeled PFUnDA, and $^{13}C_2$-labeled perfluorododecanoic acid (PFDoDA) was obtained from Wellington Laboratories (Guelph, ON, Canada). $^{13}C_{12}$-2,3,3′,5,5′-penta-

Received: June 23, 2012
Revised: September 12, 2012
Accepted: September 18, 2012
Published: October 3, 2012

Table 1. Quality Assurance for PFCAs Analysis in Food Samples

compound	(carbon atoms)	quantification (confirmation) ECNI	quantification (confirmation) EI	instrument detection limit[a] (pg) ECNI	instrument detection limit[a] (pg) EI	recovery and (reproducibility) % (SD%)[b] (n = 10, fortified)[c]	relative detector response[d] % (SD %) (n = 6, fortified)[d]	procedural blank (SD) (pg g^{-1}), n = 6	method detection limit[e] (pg g^{-1})
PFOA	(C8)	413 (414)	504 (485)	0.003	0.2	97 (16)	95 (2.8)	5 (0.4)	10
PFNA	(C9)	463 (464)	554 (535)	0.003	0.2	98 (19)	93 (3.9)	2 (0.3)	4
PFDA	(C10)	513 (514)	604 (585)	0.004	0.2	91 (17)	94 (4.9)	1 (0.3)	2
PFUnDA	(C11)	563 (564)	654 (635)	0.004	0.2	94 (18)	92 (6.3)	1.5 (0.4)	3
PFDoDA	(C12)	613 (614)	704 (685)	0.005	0.4	90 (18)	89 (7.7)	1 (0.2)	2
PFTrDA	(C13)	663 (664)	754 (735)	0.005	0.4	93 (16)		1 (0.2)	2
PFTeDA	(C14)	713 (714)	785 (786)	0.007	2	93 (17)		1 (0.4)	2

[a]1 μL injection. [b]SD: standard deviation. [c]The recoveries of the PFCAs were examined by spiking 100 pg of each standard compound into 10 composite dietary samples before extraction. [d]$^{13}C_4$-labeled PFOA, $^{13}C_5$-labeled PFNA, $^{13}C_2$-labeled PFDA, $^{13}C_2$-labeled PFUnDA, and $^{13}C_2$-labeled PFDoDA were derivatized and were fortified at 100 pg to food extracts. Matrix effects are expressed as relative detector responses (%) to the signal area responses of corresponding solvent-based preparations. [e]Food sample of 1 g. The method detection limit is defined as the concentration that produces a signal three times that of the blank. The mean blank signal was subtracted from the calculated sample concentration.

chlorobiphenyl (CB-111) was obtained from Cambridge Isotope Laboratories (Andover, MA)

2.2. Sample Collection. Diet samples from the Kyoto University Human Specimen Bank[10,11] were used for the evaluation. At the time of collection, participants were requested to donate duplicate samples of all food and drink items that they consumed over a 24-h period. These samples are referred to as duplicate 24-h diet samples. Two hundred duplicate 24-h diet samples were collected from the following locations: Hokkaido (Japan) in 1992 and 1995, Okinawa (Japan) in 1992 and 1995, Kyoto (Japan) in 1996 and 1997, Beijing (China) in 1993 and 2009, and Seoul (Korea) in 1994 and 2007.[10,12] In addition, 100 duplicate 24-h diet samples (i.e., a typical day's worth of food and drink) were purchased by volunteers from markets in Kyoto, Okinawa, and Hokkaido in 2009. The study populations were the same as those in earlier studies.[13,14] This gave a total of 300 duplicate 24-h diet samples. All food and drink samples in each duplicate sample were mixed together and homogenized. Then the 300 homogenized diet samples were combined into 60 groups (150 g), referred to as the composite dietary samples, each containing five samples (30 g) from the same location and sampling year. This process is detailed in Figure S1 of the Supporting Information. The composite dietary samples were then stored in glass bottles at −30 °C. The study protocol was approved by the Ethics Committee of Kyoto University (Kyoto, Japan). Written informed consent was obtained from all study participants.

2.3. Extraction of the Composite Dietary Samples. Each of the composite dietary samples was subjected to an ion-pair extraction. Briefly, approximately 1 g of each composite dietary sample and an internal standard mixture (100 pg of each $^{13}C_4$-labeled PFOA, $^{13}C_5$-labeled PFNA, $^{13}C_2$-labeled PFDA, $^{13}C_2$-labeled PFUnDA, and $^{13}C_2$-labeled PFDoDA) were placed in a 15-mL polypropylene centrifugation tube. Next, 1 mL of 0.5 mol L^{-1} tetrabutylammonium/0.25 mol/L sodium carbonate buffer (pH adjusted to 10 using NaOH) and 1 mL of MTBE were added to the samples, and the tubes were vortex mixed for 60 m. The samples were then centrifuged at 9840g for 5 min. The organic layer was separated twice and placed in a clean glass tube, then dried under a gentle stream of nitrogen. The residue was redissolved in 100 μL of 0.1 mol L^{-1} benzyl bromide/acetone solution containing 1 ng of 11H-perfluoroundecanoic acid and 1 ng of $^{13}C_{12}$-labeled CB111 to monitor the derivatization efficiency. The solution was then derivatized at 60 °C for 1 h. No further cleanup was conducted. Derivatized samples were analyzed by GC/MS within 24 h.

2.4. Instruments and Quantification. Derivatized PFOA, PFNA, PFDA, PFUnDA, PFDoDA, PFTrDA, and perfluorotetradecanoic acid (PFTeDA) were analyzed by GC/MS in scan mode with selected ion monitoring (Agilent 6890GC/5973MSD inert, Agilent Technologies Japan, Ltd., Tokyo, Japan). PFCAs were dissolved in 100 μL of 0.1 mol L^{-1} benzyl bromide/acetone solution and derivatized at 60 °C for 60 min with 1 ng of 11H-perfluoroundecanoic acid and 1 ng of $^{13}C_{12}$-labeled CB111 to monitor the derivatization efficiency. After benzylation, the stability was investigated by monitoring the peak area ratio over 24 h. PFCA benzyl esters were separated on a DB-5MS column (30 m length, 0.25 mm i.d., 1 μm film thickness; Agilent Technologies Japan, Ltd.) with a helium carrier gas (99.9999% purity; Air Liquide Japan Ltd., Tokyo, Japan). Splitless injections (1 μL) were performed with an injector temperature of 220 °C, and the split vent was opened after 1.5 min. The initial oven temperature was 70 °C for 2 min, after which it was increased to 100 °C at 20 °C min^{-1}, and then to 280 at 30 °C min^{-1}. To compare the limits of detection, both ECNI and EI were used to quantify the PFCA benzyl esters. In ECNI, methane (99.9999% purity; Air Liquide Japan Ltd.) was used as the reagent gas (2 mL min^{-1}). The ion source temperature was maintained at 150 °C. In EI, the ion source temperature was maintained at 250 °C. The target ions for determination of PFCAs in both ECNI and EI are summarized in Table 1.

Standard stock solutions (2 μg mL^{-1}) were diluted to seven working standard solutions (4, 2, 1, 0.8, 0.4, 0.2, and 0.1 ng mL^{-1}) by serial dilution with acetone. All the standard solutions were stored in a refrigerator at 4 ± 2 °C for a maximum period of 3 months from the date of preparation. Quantification was conducted using an internal standard dissolved in acetone. $^{13}C_4$-labeled PFOA, $^{13}C_5$-labeled PFNA, $^{13}C_2$-labeled PFDA, $^{13}C_2$-labeled PFUnDA, and $^{13}C_2$-labeled PFDoDA were used as internal standards for the PFCAs. These standards were diluted to 1 ng mL^{-1}. The instrumental detection limit (IDL) is defined as the mass of the analyte producing a peak with a signal-to-noise ratio of three. Because blank levels were larger for shorter-chain PFCAs than for longer-chain PFCAs, the final net IDLs of the shorter- and longer-chain PFCAs were nearly equivalent.

2.5. Method Detection Limits (MDLs), Blank Contamination, Total Extraction Recovery, and Possible Matrix

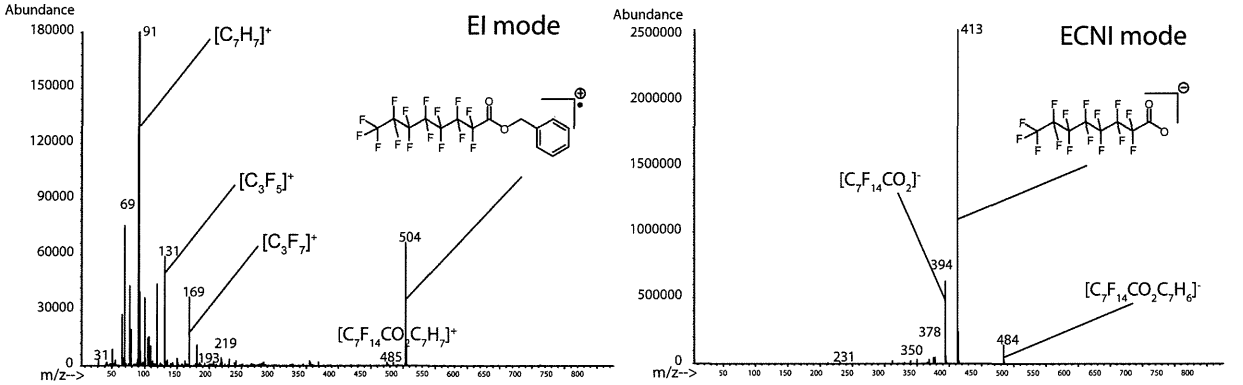

Figure 1. Mass spectra of PFOA benzyl ester in EI mode and ECNI mode (m/z 30–800).

Effect. Milli-Q water (Millipore, Billerica, MA) was used as the procedural blank control, and was analyzed after every 10 samples (n = 6). The procedural blank was extracted using the process described above, and six replicate procedural blanks were prepared independently. In this study, we observed blank contamination for all PFCAs (Table 1). The MDL is defined as the concentration that produces a signal three times that of the blank. The mean blank signal was subtracted from the calculated sample concentration (Table 1). The recoveries of the PFCAs were examined by spiking 100 pg of each standard compound into 10 composite dietary samples before extraction. Possible matrix effects on the GC-MS detector response were evaluated by comparing the response factors of PFCA benzyl esters in acetone and in food extracts prepared in acetone. The ^{13}C-labeled internal standards (100 pg) were derivatized in acetone before being used for spiking, and then added to the food extracts.

2.6. Statistical Analysis. All statistical analyses were conducted using SPSS (Version 16.0 for Windows 2007, IBM Corporation, Armonk, NY). Values of $p < 0.05$ were considered statistically significant. Concentrations lower than the detection limits were given a value of half the detection limit for statistical analyses. Statistical analyses were conducted after logarithmic transformation of the PFCAs concentrations. When the statistical tests by two-way ANOVA were significant, analysis of covariance was used to demonstrate the effect of time or location and their interactions influenced on the PFCA levels in the food composite samples.

3. RESULTS AND DISCUSSION

3.1. Quantification and Quality Assurance. *Derivatization, Mass Spectra, and IDL.* In the present study, we developed a very simple yet sensitive method for PFCAs analysis in food using GC-ECNI-MS with benzyl esterification. Benzyl esterification was used for PFCAs analysis because stabilization of the benzyl radical leaving group preferentially gives carboxylic anions of PFCAs in ECNI.[15] The PFCAs extracted from the composite dietary samples were dissolved in benzyl bromide/acetone solution and derivatized with 11H-perfluoroundecanoic acid and $^{13}C_{12}$–CB-111 (Section 2.3). Peak area ratios to $^{13}C_{12}$–CB-111 showed that the derivatization reaction time of 60 min at 60 °C was sufficient for benzylation to reach completion. After benzylation, the peak area ratios did not change significantly over 24 h (arithmetic mean ± relative standard deviation: 104 ± 5.6%, n = 10).

Mass spectra of the standard solutions were initially acquired in full-scan mode with EI or ECNI to determine the retention times and fragmentation patterns. In EI mode, the molecular ion $[M]^+$ of PFOA benzyl ester was observed at m/z 504 (Figure 1). In ECNI mode the PFOA benzyl ester showed an abundant fragment ion $[M - C_7H_7]^-$ at m/z 413 (Figure 1), corresponding to a carboxylate anion ($C_7F_{15}COO^-$). Similar fragmentation was observed among the PFCA benzyl esters with different chain lengths (ECNI mode, Figure S2; EI mode, Figure S3). As shown in Table 1, other PFCA benzyl esters also gave abundant fragment ions $[M - C_7H_7]^-$ in ECNI mode, and the IDLs ranged from 0.003 to 0.007 pg. Therefore, ENCI was used for quantification of PFCA benzyl esters in subsequent experiments.

Extraction. To avoid freeze-drying the samples and to simplify the method, the PFCAs from the composite dietary samples were extracted by ion-pair extraction[15] into an organic solvent (MTBE). This method prevented coextraction of water from the food sample.[7] The presence (or absence) of matrix effects on the GC-MS detector response was examined by spiking the food sample extracts with derivatized internal standards immediately before injection into the GC-MS (Section 2.5). The food extracts displayed only minor suppression of the internal standards (95–89% of solvent based standards) (Table 1). Because no large interferences were observed in the chromatogram in ECNI mode (Table of Contents Art), sample cleanup was not performed after ion-pair extraction.

Blank Contamination and MDLs. A widely reported problem in ultratrace analysis of PFCAs is contamination of procedural blanks.[7,16] To overcome this problem, all disposable laboratory equipment was sonicated in methanol, and the methanol was analyzed to determine potential sources of contamination. None of the laboratory equipment contributed to background levels of any analyte. The purity of each solvent was tested by evaporating 10 mL of the solvent to dryness. Artifacts originating from the evaporation procedure were investigated by comparing drying the solvent under nitrogen gas and vacuum. Comparable results were obtained with both methods. When the solvents were tested, HPLC-grade MTBE was found to contain low levels of target analytes. Therefore, the HPLC-grade MTBE was distilled by rotary evaporation to reduce the levels of contaminants. The final procedural blank levels were 5 pg g^{-1} for PFOA, 2 pg g^{-1} for PFNA, 1 pg g^{-1} for PFDA, 1.5 pg g^{-1} for PFUnDA, and 1 pg g^{-1} for PFDoDA, PFTrDA, and PFTeDA.